Author Manuscript

Author Manuscript

Author Manuscript

Author Manuscript

HHS Public Access

Author manuscript

Cell. Author manuscript; available in PMC 2020 November 27.

Published in final edited form as:

Cell. 2019 November 27; 179(6): 1276–1288.e14. doi:10.1016/j.cell.2019.10.034.

GPR146 Deficiency Protects Against Hypercholesterolemia and Atherosclerosis

Haojie Yu[1,2,3,9,*], **Antoine Rimbert**[4,5], **Alice E. Palmer**[1], **Takafumi Toyohara**[1,2,3], **Yulei Xia**[2], **Fang Xia**[2], **Leonardo M. R. Ferreira**[2,6], **Zhifen Chen**[1,2,3], **Tao Chen**[2], **Natalia Loaiza**[4], **Nathaniel Brooks Horwitz**[6], **Michael C. Kacergis**[7], **Liping Zhao**[7], **BIOS Consortium**, **Alexander A. Soukas**[7], **Jan Albert Kuivenhoven**[4], **Sekar Kathiresan**[7,8], **Chad A. Cowan**[1,2,3,*]

[1]Department of Medicine, Division of Cardiology, Beth Israel Deaconess Medical Center (BIDMC), Harvard Medical School, Boston, MA 02215, USA. [2]Department of Stem Cell and Regenerative Biology, Harvard University, Cambridge, MA 02138, USA. [3]Harvard Stem Cell Institute, Harvard University, Cambridge, MA 02138, USA. [4]Department of Pediatrics, Section Molecular Genetics, University of Groningen, University Medical Center, Antonius Deusinglaan 1, 9713 AV, Groningen, The Netherlands. [5]Institute of Thorax, INSERM, CNRS, UNIV Nantes, Nantes, 44007, France. [6]Department of Molecular and Cellular Biology, Harvard University, Cambridge, MA 02138, USA. [7]Center for Genomic Medicine, Massachusetts General Hospital, Boston, MA 02114, USA. [8]Cardiovascular Disease Initiative of the Broad Institute of Harvard and MIT, Cambridge, MA 02142, USA. [9]Lead Contact

SUMMARY

Although human genetic studies have implicated many susceptible genes associated with plasma lipid levels, their physiological and molecular functions are not fully characterized. Here we demonstrate that orphan G protein-coupled receptor 146 (GPR146*)* promotes activity of hepatic sterol regulatory element binding protein 2 (SREBP2) through activation of the extracellular signal-regulated kinase (ERK) signaling pathway, thereby regulating hepatic very low-density lipoprotein (VLDL) secretion, and subsequently circulating low-density lipoprotein cholesterol (LDL-C) and Triglycerides (TG) levels. Remarkably, GPR146 deficiency reduces plasma cholesterol levels substantially in both wild-type and LDL receptor (LDLR)-deficient mice. Finally, aortic atherosclerotic lesions are reduced by 90% and 70%, respectively, in male and female LDLR-deficient mice upon GPR146 depletion. Taken together, these findings outline a regulatory role for the GPR146/ERK axis in systemic cholesterol metabolism and suggest that GPR146 inhibition could be an effective strategy to reduce plasma cholesterol levels and atherosclerosis.

[*]Correspondence: hyu3@bidmc.harvard.edu (H.J.Y.), ccowan@bidmc.harvard.edu (C.A.C.).

AUTHOR CONTRIBUTIONS

Conceptualization, H.Y. and C.A.C.; Methodology, H.Y., J. A. K., S.K. and C.A.C.; Formal Analysis, H.Y., A. R., J. A. K. and C.A.C.; Investigation, H.Y., A. R., A.E.P., Y.X., T.T, F.X., L.M.R.F., Z.C., T.C., N.L., N.B.H., M.C.K., L.Z., A.A.S. J. A. K. and C.A.C.; Writing-Original Draft, H.Y. and C.A.C.; Writing-Review & Editing, H.Y., N.B.H. and C.A.C.; Visualization, H.Y. and C.A.C.; Supervision, C.A.C.; Funding Acquisition, C.A.C.

DECLARATION OF INTERESTS

C.A.C. is a founder of CRISPR Therapeutics and Sana Biotechnology. S.K. is a founder of Maze Therapeutics, Verve Therapeutics, and San Therapeutics.

Author Manuscript Author Manuscript Author Manuscript Author Manuscript

Graphical Abstract

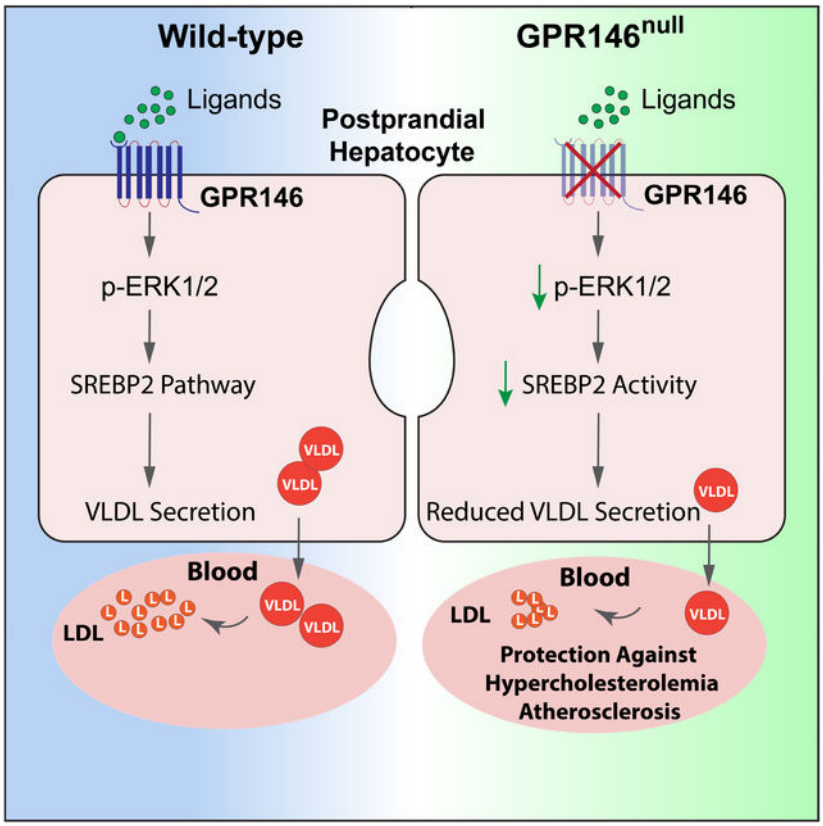

In Brief

An orphan G protein-coupled receptor, GPR146, regulates plasma cholesterol levels via ERK signaling and targeting GPR146 in mice reduces both plasma cholesterol levels and atherosclerotic lesions independently of an intact LDL receptor.

INTRODUCTION

Atherosclerotic cardiovascular disease remains the leading cause of death worldwide, and elevated plasma LDL-C and TG levels are major risk factors (Defesche et al., 2017; Do et al., 2013; Hegele, 2009; Hokanson and Austin, 1996; Rader, 2016). While lipid-lowering treatments such as statins and PCSK9 inhibitors effectively reduce plasma LDL-C levels in general, they only lead to a modest reduction of circulating TG levels. Patients with homozygous familial hypercholesterolemia (HoFH, *LDLR* mutations in both alleles) have markedly diminished response to both therapies as their lipid-lowering effects require upregulation of LDLR activity (Cuchel et al., 2014; Defesche et al., 2017).

HoFH is a rare but life-threatening genetic disorder characterized by substantially raised circulating levels of LDL-C and extremely high risk of premature atherosclerotic cardiovascular disease. Genetic studies have revealed that over 95% of HoFH patients have loss-of-function mutations in both *LDLR* alleles (Defesche et al., 2017). Conventional

Author Manuscript Author Manuscript Author Manuscript Author Manuscript

therapies to lower circulating LDL-C levels are not sufficient to reach treatment goals, and lipoprotein apheresis is usually recommended for HoFH patients. Thus, development of additional LDL-lowering drugs acting independently of LDLR activity is urgently needed to address the unmet medical needs for HoFH.

Human genetic studies have been successfully used to inform and validate new therapeutic targets, such as the development of PCSK9 inhibitors to reduce plasma LDL-C levels. There are over 300 loci uncovered to be associated with plasma lipid levels in humans (Klarin et al., 2018; Liu et al., 2017; Teslovich et al., 2010; Willer et al., 2013). However, their molecular functions are not fully characterized. Here we study the function of *GPR146*, a susceptible gene associated with plasma total cholesterol (TC), LDL-C and high density lipoprotein cholesterol (HDL-C) levels, in regulation of systemic cholesterol metabolism. In line with human genetic findings showing that GPR146 promotes plasma cholesterol levels, depletion of GPR146 in mice reduces circulating LDL-C levels substantially, which, in turn, protects against atherosclerosis. Mechanistic studies of GPR146's molecular function reveal that it promotes ERK1/2 signaling in hepatocytes upon feeding or short period of fasting, thereby increasing SREBP2 activities and VLDL secretion rate. Remarkably, the LDL-lowering effect upon GPR146 depletion does not require LDLR activity, indicating that targeting GPR146 might be an efficient strategy to treat hypercholesterolemia and atherosclerosis, particularly in HoFH, which by far lacks effective medical treatment.

RESULTS

GPR146 Regulates Plasma Cholesterol Levels in Both Human and Mouse

Human genetic studies have unequivocally established *GPR146* as a susceptible gene regulating plasma cholesterol levels. The alternative allele of a common variant (rs1997243-G), located 11-kb upstream of *GPR146*, has been shown to be associated with increased plasma TC, HDL-C and LDL-C levels in humans (Klarin et al., 2018; Liu et al., 2017; Willer et al., 2013) (Figure 1A and Table S1). This variant is in strong linkage disequilibrium (r^2= 0.989 in non-Finnish European population) with a coding variant of GPR146 (rs11761941: p.Gly11Glu) (Figure 1A). In addition, rs1997243-G is associated with an increased expression of *GPR146* in human blood (analyzed in 2,116 blood samples from the Biobank-based integrative omics study (BIOS)) (Figure 1B). Taken together, these data suggest that GPR146 is likely to promote circulating cholesterol levels in humans.

As G protein-coupled receptors (GPCRs) represent attractive targets for therapeutic drug discovery, and the physiological function of GPR146 has not been elucidated, we next examined the function of GPR146 with respect to systemic cholesterol metabolism. The CRISPR/Cas9 system (Wang et al., 2013; Yang et al., 2013) was employed to generate whole-body knockout ($Gpr146^{-/-}$) and floxed ($Gpr146^{fl/fl}$) mouse models (Figure 1C and S1A and S1B). *Gpr146* mRNA was highly expressed in liver and epididymal white adipose tissue of chow-fed wild-type ($Gpr146^{+/+}$) mice and was not detectable in $Gpr146^{-/-}$ mice (Figure 1D). $Gpr146^{-/-}$ mice were viable, fertile and normal in appearance. Mating between $Gpr146^{+/-}$ mice produced offspring in the expected Mendelian 1:2:1 ratio. In line with human genetic findings showing that increased expression of GPR146 is associated with elevated plasma TC levels, plasma TC levels were significantly reduced by 20% in male and

Author Manuscript Author Manuscript Author Manuscript Author Manuscript

by 25% in female *Gpr146*$^{-/-}$ mice fed chow compared to *Gpr146*$^{+/+}$ littermates (16-hour fasted, 16-week old male: 63.9 ± 7.3 mg/dl vs 80.4 ± 6.8 mg/dl; 16-week old female: 50.4 ± 4.8 mg/dl vs 66.9 ± 8.5 mg/dl) (Figure 1E and 1H). Fast Protein Liquid Chromatography (FPLC) analysis of pooled plasma from chow-fed mice revealed that HDL-C, LDL-C and very low density lipoprotein cholesterol (VLDL-C) were reduced by ~15%, ~35% and ~25%, respectively (Figure 1F, 1G, 1I and 1J). Consistent with the reduction in LDL-C levels, the total circulating APOB100 levels were lower in *Gpr146*$^{-/-}$ mice compared to *Gpr146*$^{+/+}$ littermates (Figure S1C and S1D). It has been well established that LDL particles consists of several subclasses with different sizes, and the small dense LDL particles are more atherogenic compared to large buoyant LDL particles (Ai et al., 2010; Ivanova et al., 2017). Importantly, by measuring APOB100 levels in different LDL fractions purified via FPLC, we found the greatest reduction of APOB100 in fraction containing small size LDL particles (Figure S1E and S1F). In summary, these data indicate that GPR146 plays a consistent role in regulation of circulating cholesterol levels in human and mouse.

Of note, reduced plasma TC levels in *Gpr146*$^{-/-}$ mice also occurred upon 6-hour fasting or 6-hour refeeding following a 16-hour fasting (Figure S1G and S1H). Moreover, as high fat, high cholesterol western-type diet is one of the main risk factors for cardiovascular diseases in humans, we next examined if the cholesterol-lowering effect upon GPR146 depletion is affected by increased dietary lipid levels. Mice challenged with a western diet (WD, 0.2% cholesterol) for two weeks exhibited substantially elevated plasma TC levels compared to mice fed chow (0.02% cholesterol); and GPR146 deficiency reduced plasma TC levels by ~20% in mice fed chow and by ~30% in mice fed WD (Figure S1I), suggesting that GPR146 deficiency reduced plasma cholesterol levels more efficiently in the presence of high dietary cholesterol levels. Moreover, GPR146-deficient mice fed a high-fat diet (HFD) exhibited a ~29% reduction of plasma TC levels compared to control mice (Figure S1J). Therefore, depletion of GPR146 reduces plasma TC levels substantially upon different dietary lipid levels or different feeding conditions.

GPR146 Promotes Plasma TG Levels

In addition to reduced plasma cholesterol levels, GPR146 depletion also led to significantly reduced plasma TG levels in both male and female mice fed chow (Figure S1K and S1L) or HFD (Figure S1M). Taken together, these findings suggest that targeting GPR146 might be an effective strategy to reduce both plasma cholesterol and TG levels.

GPR146 Deficiency Reduces Hepatic SREBP2 Activity and VLDL Secretion Rate

The difference in plasma TC levels between *Gpr146*$^{-/-}$ and control mice could be due to impaired intestinal absorption, reduced hepatic cholesterol *de novo* synthesis and subsequently reduced VLDL secretion, or increased clearance by tissue uptake and biliary excretion of bile and cholesterol (Hegele, 2009). Metabolic profiling of mice fed chow showed no difference in either food/water intake or locomotor activity (Figure S2A–S2C) between *Gpr146*$^{-/-}$ and *Gpr146*$^{+/+}$ littermates. Body composition analysis revealed similar fat mass for each group of mice fed chow (Figure S2D and S2E), suggesting that diminished plasma TC levels in the absence of GPR146 is independent of adiposity. No significant difference was found in TC/TG contents of fecal excretions between *Gpr146*$^{-/-}$ and

Author Manuscript Author Manuscript Author Manuscript Author Manuscript

Gpr146$^{+/+}$ littermates fed either chow or HFD for 3 weeks (Figure S2F–S2I). Therefore, differential intestinal absorption is unlikely to be the primary reason for the reduced plasma TC levels in GPR146-deficient mice. Given equal intestinal absorption, plasma steady-state TC levels reflect the hepatic secretion of VLDL, disposal of LDL and chylomicron remnants in the periphery and liver, and HDL-induced reverse cholesterol transport and biliary excretion (Hegele, 2009). Quantitative real-time PCR (qRT-PCR) revealed no difference in hepatic expression of HDL biosynthetic genes *Apoa1* and *Abca1* between *Gpr146*$^{-/-}$ and *Gpr146*$^{+/+}$ control mice (Figure S2J). In addition, the expression of heterodimeric ABC transporter ABCG5/G8, which mediates biliary cholesterol secretion at the apical membrane of hepatocytes (Graf et al., 2003; Yu et al., 2002), was not impaired in GPR146-deficient mice (Figure S2J). To test if reduced circulating TC/TG levels is due to enhanced chylomicron catabolism rate, we performed a lipid tolerance assay by orally delivering a dose of olive oil into mice and followed the plasma TG levels for 4 hours. No significant difference was observed in dynamic changes of plasma TG levels between *Gpr146*$^{+/+}$ and *Gpr146*$^{-/-}$ mice (Figure S2K). To measure hepatic VLDL secretion, Poloxamer-407 (an effective inhibitor of VLDL disposal by inhibiting lipoprotein lipase activity) was administered in mice, and plasma TG and TC were monitored for two hours. Both chow-fed male and female GPR146-deficient mice displayed significantly reduced TG and cholesterol secretion rates (Figure 2A and 2B, S2L and S2M) compared to wild-type littermates. Importantly, liver contents of TG/TC in *Gpr146*$^{-/-}$ mice were similar to *Gpr146*$^{+/+}$ control mice fed chow, suggesting that the hepatic TG/TC homeostasis is well maintained despite reduced VLDL secretion rate (Figure S3C–3F). Hepatic VLDL secretion rate is determined by multiple factors, such as free fatty acid (FFA) influx to the liver, hepatic *de novo* TC/TG synthesis rate and VLDL packaging (Adiels et al., 2008; Barrows and Parks, 2006). Given the fact that GPR146 is most highly expressed in white adipose tissue in both human and mouse (Figure 1D), it is possible that GPR146 regulates hepatic VLDL secretion by modulating lipolysis in adipose tissue and subsequently FFA influx to the liver. To test this hypothesis, we knocked out *Gpr146* specifically in adipocytes by crossing *Gpr146*$^{fl/fl}$ with *Adipoq*-Cre^{+} mice (Figure S2N). However, no difference in plasma TC levels was observed between *Adipoq*-Cre^{+} *Gpr146*$^{fl/fl}$ mice and control littermates (Figure S2O and S2P), suggesting that adipocyte-resident GPR146 does not regulate circulating cholesterol levels. In contrast, we also knocked out *Gpr146* specifically in hepatocytes by crossing *Gpr146*$^{fl/fl}$ with *Alb*-Cre^{+} mice (Figure S2Q), and hepatocyte-specific GPR146 depletion in *Alb*-Cre^{+} *Gpr146*$^{fl/fl}$ mice substantially reduced plasma TC levels by ~20% (male: 74.2 ± 6.1 mg/dl vs 61.2 ± 6.4 mg/dl; female: 61.8 ± 6.1 mg/dl vs 48.4 ± 3.2 mg/dl) compared to control littermates (Figure 2E). Consistently, hepatic VLDL-TG/TC secretion rates were significantly reduced in *Alb*-Cre^{+} *Gpr146*$^{fl/fl}$ mice compared to control littermates (Figure 2C and 2D). To further demonstrate that GPR146 directly regulates hepatic VLDL secretion, we employed an ELISA-based assay to measure secreted levels of APOB100, the structural protein on VLDL particles, in human hepatoma Huh7 cells. In line with the *in vivo* findings, CRISPR/Cas9-mediated depletion of GPR146 in Huh7 cells led to 30% less secreted APOB100 levels than that in control cells (Figure 2F, S2R and S2S), while recombinantly overexpressed GPR146 significantly increased secreted APOB100 levels (Figure 2G and S2U). Moreover, depletion of GPR146 in Huh7 cells has no effect on uptake of LDL particles (Figure S2T). Taken together, these data show that GPR146 in hepatocyte plays a

Author Manuscript Author Manuscript Author Manuscript Author Manuscript

regulatory role in VLDL metabolism, and that reduced plasma LDL-C and TG levels in *Gpr146*$^{-/-}$ mice are very likely due to decreased hepatic VLDL secretion rate.

Despite reduced hepatic VLDL secretion rate, mRNA levels of known genes that are involved in regulation of hepatic VLDL assembly and secretion, such as *Mttp*, *Apob*, *Dgat1*, *Dgat2* and *Sort1*, were unchanged in GPR146-deficient mice compared to wild type littermates (Figure S2J). To further determine the underlying molecular mechanism by which GPR146 regulates hepatic VLDL secretion, we performed transcriptome analysis (GEO: GSE139082) of liver from refed male mice upon chow feeding (6-hour refeeding after a 16-hour fast). To further identify signaling pathways regulated by GPR146, we performed unbiased gene set enrichment analysis (GSEA) by using three different databases, namely Reactome pathway gene sets, Hallmark gene sets and KEGG pathway gene sets, all of which revealed that the cholesterol biosynthesis pathway was significantly downregulated in liver of GPR146-deficient mice compared to wild-type littermates (Figure 2H, 2I, S3A and S3B). Results were further confirmed by quantitative real-time PCR (qRT-PCR). Livers from male *Gpr146*$^{-/-}$ mice showed decreased mRNA levels of *Hmgcr* encoding the rate-limiting enzyme for cholesterol biosynthesis, as well as decreased mRNA levels of *Hmgcs1* and *Pmvk* (Figure 2J). We also measured mRNA levels of cholesterol biosynthetic genes in livers of refed female mice, and found downregulation of many genes including *Hmgcr*, *Hmgcs1*, *Pmvk*, *Mvk* and *Mvd* (Figure 2J). In line with downregulated hepatic cholesterol biosynthesis pathway upon GPR146 depletion, protein levels of the mature SREBP2, the master transcriptional regulator of cholesterol biosynthesis (Horton et al., 2002; Rong et al., 2017), were significantly decreased in liver of *Gpr146*$^{-/-}$ male mice (Figure 2K and 2L). Protein levels of SREBP2 target genes, such as *Hmgcr, Hmgcs1* and *Ldlr*, were also significantly reduced in the absence of GPR146 (Figure 2K and 2L). There is longstanding evidence that hepatic SREBP2 plays an essential role in regulating whole body cholesterol homeostasis. Liver-specific depletion of SREBP2 or abolishment of its activity via depletion of SREBP cleavage-activating protein (SCAP) led to significantly reduced hepatic cholesterol synthesis rate, and subsequently decreased hepatic cholesterol pool and VLDL secretion levels (Matsuda et al., 2001; Moon et al., 2012; Rong et al., 2017). While liver TC concentrations were similar between *Gpr146*$^{+/+}$ mice and *Gpr146*$^{-/-}$ littermates upon chow feeding, there was a trend towards reduction in male *Gpr146*$^{-/-}$ mice and a significant decrease in female *Gpr146*$^{-/-}$ mice upon western diet feeding for two months, compared to control littermates (Figure S3C and S3D). Therefore, the major mechanism responsible for reduced plasma LDL-C levels in *Gpr146*$^{-/-}$ mice is likely due to decreased hepatic VLDL secretion, secondary to a downregulation of SREBP2 signaling pathway in liver.

GPR146 Signaling Promotes ERK1/2 Activities in Hepatocytes Upon Feeding

We next asked how GPR146-activated signaling cascade regulates the cholesterol biosynthesis pathway in liver. Downregulation of cholesterol biosynthetic genes in the absence of GPR146 was observed under fasting-refeeding conditions, but not in mice after a prolonged 16-hour fasting (Figure S2V). Abundant evidence demonstrates that hepatic SREBP2 activity and expression of its target genes such as *HMGCR* and *LDLR* fall while fasting and rise substantially upon refeeding, suggesting the existence of feeding-responsive signaling pathways regulating hepatic cholesterol synthesis in the presence of dietary

Author Manuscript Author Manuscript Author Manuscript Author Manuscript

nutrition (Horton et al., 1998; Liang et al., 2002; Matsuda et al., 2001; Slakey et al., 1972). Therefore, we speculated that GPR146-elicited signaling cascade is involved in the regulatory network of cholesterol synthesis upon feeding. Gene sets enrichment analysis using KEGG gene sets revealed mitogen-activated protein kinase (MAPK) signaling as one of the significantly downregulated pathways in liver of *Gpr146*$^{-/-}$ mice upon feeding (Figure 3A and S3B). Consistently, the extracellular signal-regulated kinases (ERK1/2) activities were decreased in livers from both male and female *Gpr146*$^{-/-}$ mice compared to *Gpr146*$^{+/+}$ littermates upon feeding (Figure 3B and 3C), while no significant difference was observed in mice after a prolonged 16-hour fasting (Figure 3D and 3E). Considering the fact that hepatic ERK1/2 activities are substantially increased upon feeding (Figure 3F), these data taken together suggests that GPR146 upon ligand binding stimulates ERK1/2 activities in liver upon feeding and the natural ligand of GPR146 might be regulated by feeding conditions. Moreover, it is well established that many GPCRs activate ERK1/2 signaling upon ligand binding (van Biesen et al., 1996). To further test if GPR146 directly activates ERK1/2 signaling upon 'feeding' in hepatocytes, we over-expressed human GPR146 in HepG2 cells and found substantially increased levels of phosphor-ERK1/2 compared to GFP control upon serum stimulation (Figure 3G and 3H, S4A and S4B).

GPR146 Regulates Refed SREBP2 Signaling Pathway and Plasma TC Levels Through ERK1/2

ERK1/2 signaling has been previously shown to regulate SREBP2 activity in HepG2 cells via direct phosphorylation (Arito et al., 2008; Kotzka et al., 2004; Kotzka et al., 2000). However, the *in vivo* physiological function of ERK1/2 signaling in regulation of hepatic cholesterol metabolism is unknown. Here, we sought to determine whether GPR146 regulates hepatic SREBP2 signaling pathway through ERK1/2, thereby regulating plasma cholesterol levels. Serum treatment after starvation induced transcriptional upregulation of *SREBP2* and its classic downstream genes *HMGCR* and *LDLR* in human hepatoma HepG2, Huh7 and mouse hepatocyte AML12 cells, while it was greatly attenuated after blocking MEK1/ERK1/2 pathway using the well-characterized MEK1 inhibitor PD0325901(PD) (Figure 4A–4C and S4C–S4I). In addition, protein levels of mature SREBP2 were also reduced in the presence of MEK inhibitor compared to DMSO control (Figure 4D). To rule out the possibility of MEK1 inhibitor's off-target effects, we used CRISPR/Cas9 to deplete ERK1 and ERK2 individually or ERK1/2 together in HepG2 cells and found both the basal and serum stimulated expression levels of *SREBP2*, *HMGCR* and *LDLR* were significantly reduced in the absence of ERK2, but not ERK1 (Figure 4E–4H). These data taken together suggest that ERK activities are required for full activation of SREBP2 pathway in hepatocytes upon feeding. Importantly, in line with the findings that overexpression of GPR146 upregulates ERK1/2 activities (Figure 3G and 3H), recombinant overexpression of GPR146 in HepG2 and Huh7 cells promoted the expression levels of both *HMGCR* and *LDLR* compared to GFP control upon serum stimulation (Figure 4I and S4J).

Given the observation that depletion of GPR146 is associated with downregulated SREBP2 signaling pathway, as well as drastically diminished ERK1/2 activity in liver from refed mice, we next asked a critical question: is the cholesterol-lowering effect upon GPR146 depletion due to reduced ERK1/2 activity *in vivo*? *Gpr146*$^{+/+}$ and *Gpr146*$^{-/-}$ female mice

Author Manuscript Author Manuscript Author Manuscript Author Manuscript

fed chow were treated with MEK1 inhibitor PD0325901 for 14 days before measuring plasma TC levels. Mice upon PD0325901 administration exhibited significantly reduced refed phosphor-ERK1/2 (pERK1/2) levels in liver, but not reduced levels of other MAPK families, such as phosphor-JNK and phosphor-P38 (Figure 4J, S4K and S4L). Consistent with a previous study that MEK/ERK inhibition in mice led to substantially reduced plasma cholesterol levels (Ozaki et al., 2016), PD0325901 significantly reduced plasma TC levels by ~22% in *Gpr146*$^{+/+}$ (C57BL/6) mice (vehicle vs PD: 66.4 ± 5.4 mg/dl vs 51.8 ± 7.8 mg/dl), while it had no additional effect in *Gpr146*$^{-/-}$ mice compared to vehicle control (vehicle vs PD: 53.1 ± 5.4 mg/dl vs 55.8 ± 1.9 mg/dl) (Figure 4K), strongly suggesting reduction of ERK1/2 activity as a key mechanism for decreased plasma TC levels in *Gpr146*$^{-/-}$ mice. Furthermore, in line with *in vitro* findings that ERK1/2 signaling cascade is required for promoting the activity of SREBP2 in hepatocytes upon 'feeding', mRNA levels of *Srebp2* and its target genes *Hmgcr* and *Ldlr* in liver were significantly reduced in wild-type mice but not in *Gpr146*$^{-/-}$ mice after 6-hour refeeding upon MEK1/ERK1/2 inhibition (Figure 4L).

To further explore the effects of MEK1/ERK inhibition on plasma TC levels, we tested if a single dose of PD0325901 could acutely abolish refeeding-induced upregulation of ERK1/2 activities, thereby reducing plasma TC levels in mice (Figure S4M). PD0325901 treatment exhibited a dose-dependent reduction of refed pERK1/2 levels in liver of 14-week old mice (Figure S4N and S4O). Consistent with *in vitro* findings that ERK activities are required for full activation of SREBP2 pathway in hepatocytes upon feeding, mRNA levels of cholesterol biosynthetic genes, such as *Srebp2, Hmgcr, Mvd* and *Ldlr*, were downregulated in liver treated with PD0325901 compared to vehicle control (Figure S4P). Importantly, PD0325901 treatment reduced plasma TC levels in a dose-dependent manner (vehicle vs PD 5mg/kg vs PD 10mg/kg: 86.3 ± 7.6 mg/dl vs 77.2 ± 4.7 mg/dl vs 68.4 ± 9.7 mg/dl) (Figure S4Q). Consistently, a single dose of PD0325901 treatment (10 mg/kg) significantly reduced plasma TC levels in 24-week old mice (Figure S4R). All these *in vitro* and *in vivo* data together suggest that ERK1/2 plays a role in cholesterol metabolism, and GPR146 regulates hepatic SREBP2 activities and plasma cholesterol levels through, at least in part, the ERK1/2 signaling cascade.

GPR146 Regulates ERK/SREBP2 Axis in Mice upon Short Period of Fasting

Based on the observation that GPR146 deficiency led to diminished activities of ERK1/2 and SREBP2 only in a fasting-refeeding paradigm (6-hour refeeding after a 16-hour fast), not upon prolonged fasting (16-hour fasting), we speculated that upregulated activities of ERK1/2 and SREBP2 upon feeding would gradually descend to baseline during prolonged fasting, and the GPR146/ERK/SREBP2 axis might still be in operation during early hours of fasting (6-hour fasting). Following the fasting-refeeding regimens (Figure 5A), we first confirmed that hepatic ERK1/2 activities decreased over time during fasting (Figure 5B and Figure 5C). We further found that pERK1/2, precursor and mature SREBP2 protein levels were significantly reduced in liver of GPR146-deficient mice compared to control littermates upon 6-hour fasting (Figure 5D and 5E). Consistently, mRNA levels of many cholesterol biosynthetic genes in liver were downregulated in the absence of GPR146 (Figure 5F). Thus, these data are in consistence with our observation that plasma TC levels

Author Manuscript Author Manuscript Author Manuscript Author Manuscript

were significantly reduced in GPR146-deficient mice upon 6-hour fasting compared to control littermates.

Cholesterol-lowering Effect upon GPR146 Depletion Does Not Require LDLR Activity

Feedback suppression of SREBP2 pathway by LDLR plays a pivotal role in maintaining the balance of cholesterol levels between liver and blood (Brown and Goldstein, 1986). Defects in this regulation lead to dramatically elevated plasma LDL-C levels in HoFH patients due to increased hepatic cholesterol synthesis as well as decreased LDL-C clearance (Brown and Goldstein, 1975, 1986; Goldstein and Brown, 1973). The fact that the cholesterol-lowering effect upon GPR146 depletion was accompanied by reduced hepatic LDLR expression suggests that inhibition of GPR146 might reduce plasma cholesterol levels independent of LDLR activity. To test this hypothesis, we depleted GPR146 in mice lacking LDLR. On the chow diet, plasma TC levels were reduced by ~30% in both male and female $Gpr146^{-/-}$ $Ldlr^{-/-}$ mice compared to $Gpr146^{+/+}Ldlr^{-/-}$ littermates (Figure 6A and 6C). Remarkably, upon western diet feeding for 16 weeks, male and female $Gpr146^{-/-}$ $Ldlr^{-/-}$ mice exhibited ~60% and ~35% reductions of plasma TC levels, respectively, compared to $Gpr146^{+/+}$ $Ldlr^{-/-}$ littermates (Figure 6A, 6C and 6E). Further analysis of cholesterol levels in atherogenic VLDL/LDL fraction of plasma showed ~35% reduction in both male and female $Gpr146^{-/-}$ $Ldlr^{-/-}$ mice fed chow; and ~60% and ~35% respective reductions in male and female $Gpr146^{-/-}$ $Ldlr^{-/-}$ mice fed WD compared to control littermates (Figure 6B and 6D). Moreover, plasma TG levels were reduced by ~37% and ~50%, respectively, in male and female $Gpr146^{-/-}$ $Ldlr^{-/-}$ mice fed chow compared to $Gpr146^{+/+}$ $Ldlr^{-/-}$ littermates; and by ~77% and ~50%, respectively, in male and female $Gpr146^{-/-}$ $Ldlr^{-/-}$ mice fed WD compared to control mice (Figure S5A–S5D). Additionally, there is no difference in body weight between $Gpr146^{+/+}$ $Ldlr^{-/-}$ mice and $Gpr146^{-/-}$ $Ldlr^{-/-}$ littermate after feeding with WD for 16 weeks (Figure S5E).

We next evaluated whether depletion of GPR146 leads to reduced hepatic ERK1/2 and SREBP2 activities in mice lacking LDLR. Indeed, protein levels of pERK1/2, precursor and mature SREBP2 were substantially reduced in liver of GPR146-deficient mice compared to control littermates (Figure 6F and 6G). In addition, mRNA levels of many cholesterol biosynthetic genes in liver were downregulated in the absence of GPR146 in both male and female mice (Figure 6H). Taken together, these data suggest that the LDLR activity is not required for TC-lowering effect upon GPR146 depletion, and GPR146/ERK/SREBP2 axis is still in operation in LDLR-deficient mice upon feeding.

GPR146 Deficiency Protects Against Atherosclerosis

To determine if the lipid-lowering effects upon GPR146 depletion protects mice against atherosclerosis, we examined atherosclerotic plaques in mice lacking LDLR, the lipid profile of which more closely resembles that of dyslipidemic humans (the predominant lipoprotein is the APOB100-containing LDL). In addition, HoFH is usually characterized by accelerated atherosclerosis at a very young age (Cuchel et al., 2014; Defesche et al., 2017). Thus, we examined if the substantial reduction of atherogenic VLDL/LDL-C upon GPR146 depletion would protect $Ldlr^{-/-}$ mice against atherosclerosis. Atherosclerotic lesion area evaluated by *en face* Oil Red O staining of the full-length aorta was drastically reduced by ~90% and

Author Manuscript Author Manuscript Author Manuscript Author Manuscript

~70%, respectively, in male and female *Gpr146*$^{-/-}$ *Ldlr*$^{-/-}$ mice fed WD for 16 weeks compared to *Gpr146*$^{+/+}$ *Ldlr*$^{-/-}$ littermates (Figure 6I–6N, S6). Thus, GPR146 deficiency confers protection against atherosclerosis to mice lacking LDLR.

Knockdown of Hepatic GPR146 by AAV-delivered shRNA Lowers Plasma Cholesterol Levels in Mice Lacking LDLR

To examine if depletion of hepatic GPR146 in adult *Ldlr*$^{-/-}$ mice would substantially reduce plasma TC levels, mice were injected with AAV8-shRNA targeting GPR146 (Figure 7A). GPR146 mRNA expression level in liver was strongly reduced by 75% compared to scramble control (Figure S7A). Remarkably, plasma TC levels were reduced by ~34% and ~23%, respectively, in male and female mice treated with *Gpr146*-shRNA compared with scramble-shRNA at two weeks post-injection (Figure 7B and 7C). Upon WD feeding for four weeks, plasma TC levels were reduced by ~50% and ~30%, respectively, in male and female GPR146-depleted mice compared to control mice (Figure 7B and 7C). Moreover, cholesterol levels in VLDL/LDL fraction of plasma showed ~55% and ~32% reductions in male and female GPR146-depleted mice upon four weeks of WD feeding, respectively (Figure 7D). In line with the findings from GPR146 germline knockout mice showing downregulation of hepatic SREBP2 signaling pathway, AAV-induced depletion of GPR146 also reduced mRNA levels of many cholesterol biosynthetic genes in liver compared to scramble control (Figure 7E). Plasma TG levels were also substantially reduced by ~55% and ~25% in male and female GPR146-depleted mice compared to control littermates upon four weeks of WD feeding, respectively (Figure S7B–S7E). Taken together, these data suggest that acute depletion of GPR146 in liver of adult mice reduced plasma TC levels to a similar extent compared to germline knockout of GPR146.

DISCUSSION

Our results show that depletion of GPR146 reduces circulating cholesterol and TG levels substantially and confers great protection to LDLR-deficient mice against atherosclerosis. We further put forward a signaling pathway in which GPR146 promotes ERK1/2 signaling cascade in hepatocytes upon feeding, which in turn increases SREBP2 activities and VLDL secretion rate (Figure 7F). This study thus uncovers GPR146 as a new therapeutic target to treat hypercholesterolemia.

The Role of GPR146 in Regulation of Hepatic ERK1/2 and SREBP2 Pathways

We conclude that GPR146/ERK/SREBP2 axis starts operating upon feeding, further lasts for at least 6 hours postprandially, and eventually decreases to baseline after a prolonged fasting (16-hour fasting). This also suggests that the amount of natural ligand for GPR146 might be upregulated upon feeding, or GPR146 might cross-talk with other signaling pathways that are activated upon feeding to regulate hepatic ERK1/2 activities. It is worth noting that there remains a significant reduction of plasma TC levels in the absence of GPR146 upon a prolonged 16-hour fasting despite no changes of ERK1/2 and SREBP2 activities, which suggest that there might be other GPR146 downstream pathways modulating plasma TC levels under this condition.

Author Manuscript Author Manuscript Author Manuscript Author Manuscript

Although evidence from both *in vivo* and *in vitro* studies unequivocally demonstrated that GPR146 is required for ERK1/2 activation in hepatocytes upon feeding, the detailed signaling cascade is still under investigation. It is well documented that many GPCRs upon ligand binding activate ERK signaling and further regulate cell growth, division and differentiation (van Biesen et al., 1996). In hepatocytes, many hormones and growth factors such as epidermal growth factors (EGF) and fibroblast growth factors (FGF) are able to stimulate ERK1/2 signaling cascade (Fremin et al., 2007; Guegan et al., 2012). Gene set enrichment analysis of liver transcriptome revealed that growth hormone receptor signaling cascade was significantly downregulated upon GPR146 depletion. Therefore, the underlying mechanism by which GPR146 modulates ERK1/2 activities might be through 'direct' or 'indirect' fashions: GPR146 upon ligand binding might directly activate ERK1/2 through activated Gα and Gβγ subunits and downstream signaling cascade; or GPR146 signaling might cross-talk with other growth factor/hormone signaling pathways to modulate ERK1/2 activities. Further investigation will be needed to determine the signaling cascade of how GPR146 regulates ERK1/2 in hepatocytes.

Substantial evidence supports the conclusion that hepatic SREBP2 activity and cholesterol biosynthesis rate fall while fasting and rise greatly upon refeeding, indicating the existence of feeding-responsive signaling pathways upregulating hepatic cholesterol synthesis in the presence of dietary nutrition (Horton et al., 1998; Liang et al., 2002; Matsuda et al., 2001; Slakey et al., 1972). Through both *in vivo* and *in vitro* studies, we discovered that ERK1/2 signaling is required for upregulation of SREBP2 pathway in hepatocytes upon feeding. Inhibition of ERK1/2 reduced mRNA levels of *Srebp2*, *Hmgcr* and *Ldlr* in both *in vitro*-cultured hepatocyte and liver upon feeding. Previous studies in HepG2 cells showed that MEK1/ERK cascade directly phosphorylates SREBP2 at Ser-432 and Ser-455, which inhibits its sumoylation and subsequently promotes its transcription activity (Arito et al., 2008; Kotzka et al., 2004; Kotzka et al., 2000). Therefore, it is possible that the GPR146/ERK axis modulates SREBP2 activity through both transcriptional regulation and posttranslational modification. Moreover, there is longstanding evidence showing that, besides SREBP2, additional feeding-responsive transcription factors are likely to promote expression of cholesterol biosynthetic genes. SREBP2 may maintain promoters of target genes in a receptive state for binding of those transcription factors (Gokey et al., 2011; Liang et al., 2002). The early growth response gene family (*EGR1*, *EGR2* and *EGR3*), which are ERK1/2 target genes, have previously been indicated as additional transcription factors to upregulate cholesterol biosynthetic gene expression upon feeding (Gokey et al., 2011). We found significantly reduced expression of all three *EGR* genes in liver of GPR146-deficient mice upon feeding (data not shown). Therefore, the downregulated cholesterol biosynthesis pathway upon GPR146 depletion might be a synergistic effect by reduced expression of SREBP2 and EGR genes.

In summary, we provide several lines of evidence that the GPR146/ERK/SREBP2 axis regulates plasma cholesterol levels and depletion of GPR146 protects against hypercholesterolemia and atherosclerosis in LDLR-deficient mice. Therefore, antagonists targeting GPR146 are likely to be an efficient approach to tackle atherosclerotic cardiovascular disease in both the general population and HoFH patients.

Author Manuscript Author Manuscript Author Manuscript Author Manuscript

STAR METHODS

LEAD CONTACT AND MATERIALS AVAILABILITY

Further information and requests for resources and reagents from this study should be directed to the Lead Contact, Haojie Yu (hyu3@bidmc.harvard.edu). All unique/stable reagents generated in this study are available from the Lead Contact with a completed Materials Transfer Agreement.

EXPERIMENTAL MODEL AND SUBJECT DETAILS

***E. coli* Strain—**To reduce the frequency of homologous recombination of long terminal repeat (LTRs), *E. coli* stbl3 strain cultured in LB broth was used to clone all of the lentiviral vectors.

Mice—All animal care and experimental procedures used in this study were approved by the Institutional Animal Care and Use Committee at Harvard University and Beth Israel Deaconess Medical Center. Mice were housed under a 12-hour light-dark cycle with free access to water and normal chow diet. Both male and female 6- to 36-week-old littermate mice were used in this study to match age and sex. C57BL/6 (The Jackson Laboratory, RRID: IMSR_JAX:000664), *Albumin-Cre (*The Jackson Laboratory, RRID: IMSR_JAX: 003574)*, Adipoq-Cre* (The Jackson Laboratory, RRID: IMSR_JAX:010803) and $Ldlr^{-/-}$ (The Jackson Laboratory, RRID: IMSR_JAX:002207) mice were obtained from Jackson Laboratory at 8 weeks of age.

Gpr146 whole-body knockout ($Gpr146^{-/-}$) and *loxp/loxp* knockin mice ($Gpr146^{fl/fl}$) on C57BL/6 background were generated by using CRISPR/Cas9-based protocol previously reported (Wang et al., 2013; Yang et al., 2013). Microinjection was performed in Genome Modification Facility at Harvard University. Briefly, Cas9 mRNA (100 ng/ μl), sgRNAs (50 ng/ μl) and donor oligos (100 ng/ μl) were mixed and injected into zygotes at the pronuclei stage. Genome-edited F1 $Gpr146^{-/-}$ and $Gpr146^{+/fl}$ mice were bred with C57BL/6 mice for two rounds to dilute the off-target effects. $Gpr146^{+/+}$ and $Gpr146^{-/-}$ littermates were generated by breeding $Gpr146^{+/-}$ mice. Liver-specific or fat-specific *Gpr146* knockout mice were generated by crossing $Gpr146^{fl/fl}$ with *Albumin-Cre or Adipoq-Cre* mice, respectively. $Gpr146^{-/-}$ mice were crossed with $Ldlr^{-/-}$ mice to generate $Gpr146^{+/+}$/ $Ldlr^{-/-}$ and $Gpr146^{-/-}$/ $Ldlr^{-/-}$ mice. For studies with special diets, 14-week-old mice were placed on high-fat diet (60/Fat, TD.06414, Envigo) for a total period of 3 weeks; 14-week-old male mice were placed on western diet (TD.10885, Envigo) for a total period of 2 weeks.

The detailed schematic diagrams of generating *Gpr146* mouse models are shown in Figure S1. Sequences of guide RNAs and donor oligoes used for generating *Gpr146* whole-body knockout and *loxp/loxp* knockin mice are shown in Key Resources Table. Taqman probe Mm01951835_s1 (Life Technologies) mapping to mouse *Gpr146* coding exon was used to detect the mRNA levels in variety of tissues/organs from $Gpr146^{-/-}$ and $Gpr146^{+/+}$ mice.

Cell Lines, Culture Conditions, Transfection and Infection—The Huh7 cell line is a hepatocyte-derived carcinoma cell line that was originally taken from a liver tumor in a 57-year-old Japanese male (JCRB Cell Bank, JCRB0403). The HepG2 cell line was derived

Author Manuscript Author Manuscript Author Manuscript Author Manuscript

from a liver hepatocellular carcinoma of a 15-year-old Caucasian male (ATCC, ATCC® HB-8065™). The AML12 (alpha mouse liver 12) cell line was established from hepatocytes from a male mouse (CD1 strain, line MT42) transgenic for human TGF alpha (ATCC, ATCC® CRL-2254™). HEK293T cells were generated from human embryonic kidney 293 cells with SV40 T-antigen expression (ATCC, ATCC® CRL-3216™). AML12 cells were cultured in a 1:1 mixture of Dulbecco's modified Eagle's medium and Ham's F12 medium with 10% FBS, 0.005 mg/ml insulin, 0.005 mg/ml transferrin, 5 ng/ml selenium and 40 ng/ml dexamethasone. Huh7, HepG2 and HEK293T cells were cultured in Dulbecco's modified Eagle's medium (DMEM) supplemented with 10% fetal bovine serum (FBS) and 1% penicillin/streptomycin. All the cells were cultured in a 5% CO2 atmosphere at 37. For plasmids transfection of HEK293T cells, Lipofectamine 3000 (Thermo Fisher) reagent was used according to the manufacturer's instructions. To knock out genes in Huh7 and HepG2 cells, lentiviruses containing CRISPR lentiviral vectors were used to infect the cells for 16 hours followed by antibiotics selection for 72 hours.

METHOD DETAILS

eQTL studies—Genotype data for variant rs1997243 and normalized gene expression values for 2,116 samples from the BIOS cohort were extracted for GPR146 (Westra et al., 2013; Zhernakova et al., 2017) (http://www.bbmri.nl/acquisition-use-analyze/bios/). A Spearman correlation (conf. 0.95) was used to calculate correlation between the genotypes of rs1997243 and normalized gene expression data.

CRISPR-induced depletion of *GPR146* and *APOB100* in human hepatoma Huh7 cells—CRISPR/Cas9-based gene targeting in human hepatoma Huh7 cells was established according to previous study with modifications (Liu et al., 2017). In brief, Huh7 stable cell line expressing Cas9 was generated by infection of lentiCas9-Blast (Addgene) packaged in lentiviruses for 16 hours followed by selection with 30 μg/ml blasticidin for 72 hours. Guide RNAs targeting *GPR146* and *APOB100* were constructed into lentiviral vector lentiGuide-Puro (Addgene), and packaged viruses from HEK293T cells were used to infect Huh7 cells expressing Cas9 for 16 hours. Cells were subsequently cultured in the presence of 10 μg/ml puromycin for five days before assays. Sequences of guide RNAs used for targeting *GPR146* and *APO*B100 are shown in Table S2.

***In vitro* APOB100 secretion assay—**Huh7 cells were seeded one day before assay. And they were rinsed once with PBS before culturing for 12 hours in serum-free medium. Subsequently, the amount of secreted APOB100 in medium was measured using ELISA kit (MABTECH) according to the manufacture's instructions.

***In vitro* LDL uptake assay—**To measure LDL uptake, Huh7 cells were incubated in serum-free medium for 4 hours followed by incubation in serum-free medium containing 5 μg/ml of Dil-LDL (Thermo Fisher) for 1 hour. The cells were fixed with 4% paraformaldehyde and co-stained with DAPI for imaging. Images including 20,000 cells were taken using automated high-content microscopy Cellomics Array Scan *VTI* and cellular intensity of Dil-LDL was quantified.

Author Manuscript Author Manuscript Author Manuscript Author Manuscript

Blood lipid assays—Blood were collected from tail tips after different fasting/feeding conditions as specified, and plasma were further isolated via centrifugation. Triglyceride and total cholesterol levels were measured using Infinity Triglycerides Reagent (Thermo Fisher) and Infinity Cholesterol Reagent (Thermo Fisher) respectively according to the manufacturer's instructions. For fast protein liquid chromatography analysis, pooled plasma samples from mice fasted 16 hours was subjected to FPLC. Cholesterol was measured in the eluted fractions using Infinity Cholesterol Reagent (Thermo Fisher). For apolipoprotein analysis, equal volume of FPLC fractions were subjected to SDS-PAGE and immunoblotting against APOB. HDL and LDL/VLDL Quantitation Kit (Sigma-Aldrich) was used to separate HDL from LDL/VLDL in plasma followed by measurement of cholesterol and TG levels in those fractions.

Hepatic VLDL secretion assay—To measure the hepatic VLDL secretion rate, mice were fasted for 4 hours, followed by intraperitoneal injection of 1g/kg body weight Poloxamer-407 (Sigma). Immediate before, at 60 min, and 120 min after administration of Poloxamer-407, tail vein blood samples were taken and plasma cholesterol and TG levels were measured.

Oral lipid tolerance assay—Mice were fasted for 6 hours and then received 200 μl olive oil via oral gavage. Blood samples were taken from the tail vein right before and at different time points (0, 1h, 2h, 3h and 4h) after oral gavage. Plasma was then isolated to measure TG levels using Infinity Triglycerides Reagent (Thermo Fisher).

***En Face* quantification of Atherosclerotic lesions in the aorta—**Seven-week-old *Gpr146*$^{+/+}$/ *Ldlr*$^{-/-}$ mice and *Gpr146*$^{-/-}$/ *Ldlr*$^{-/-}$ littermates were placed on western diet (TD.10885, Envigo) for a total period of 16 weeks. Afterwards, mice were anesthetized and the aorta was carefully perfused with 10 ml of saline via the left ventricle. The heart, along with the attached full-length aorta was detached carefully and fixed in 10% formalin for 3 days. After the heart and surrounding adventitial fat tissue were removed carefully under a dissection microscope, the aorta was then opened longitudinally from the aortic root to iliac bifurcation and pinned on a black rubber plate. The aorta was treated with 60% isopropanol for 10 min before staining with oil red O solution (3 mg/ml in 60% isopropanol, filtered twice through a 0.2- μl filter) for 15 minutes and destaining with 60% isopropanol for 5 minutes to eliminate background staining. The stained aortas were stored in 10% formalin until images were captured. The oil-red O-stained atherosclerotic lesion area in full-length aorta was quantitated using the Image J software. All image capture and quantitation were done in a blinded fashion.

MEK1 inhibitor treatment—For *in vivo* therapeutic assays, PD0325901 was firstly dissolved in DMSO at a concentration of 100 mg/ml, then diluted in vehicle (0.5% hypromellose and 0.2% Tween-80) at a concentration of 0.5 mg/ml, and administered by intraperitoneal injection (5mg/kg or 10mg/kg BW) daily for the times indicated. Control mice were injected with vehicle.

For *in vitro* assays with MEK1 inhibitor, plated human Huh7 and HepG2 cells were rinsed once with PBS and further cultured in serum-free medium for 48 hours to reduce stimulating

Author Manuscript Author Manuscript Author Manuscript Author Manuscript

factors to background. Cells were then pre-treated with DMSO or 1μM PD0325901 for one hour followed by addition of Fetal bovine serum to a final concentration of 20% and incubation for the time indicated. Cells were then rinsed once with PBS before extraction of RNA or protein for analysis. For treatment with PD0325901 in AML12 cells, all the procedures are the same except that the cells were rinsed once with PBS and further cultured in serum-free, insulin-free medium for 24 hours before PD treatment.

***In vivo* knockdown of hepatic *Gpr146* using AAV-delivered shRNA—**To knock down hepatic *Gpr146 in vivo*, AAV8-scramble-shRNA (Vector Biolabs) or AAV8-*Gpr146*-shRNA (Vector Biolabs) were administered to eight-week-old $Ldlr^{-/-}$ mice via retro-orbital injection, with a dose of 6×10^{11} gc per male mouse and 4×10^{11} gc per female mouse. Heparinized blood samples were taken at 2, 4 and 6 weeks post-injection for plasma lipid analysis, western diet-feeding started at 2 weeks post-injection. Mice were sacrificed at 6 weeks post-injection and livers and plasma were collected for further analysis.

Sequences of shRNAs used for *in vivo* gene targeting are as follows.

Gpr146: GCATTATCTGGGCATCCTACA

Immunoblotting—For immunoblotting analyses, the tissues and cells were lysed in RIPA buffer containing protease and phosphatase inhibitors (Thermo Fisher). Protein levels were quantified using BCA protein assay kit (Thermo Fisher) and lysate containing equal amount of protein was subjected to SDS-PAGE, and further transferred to polyvinylidene fluoride (PVDF) membranes, followed by incubations with primary and secondary antibodies.

Immunofluorescence—To detect the recombinant expression of GPR146 with a C-terminal FLAG tag, HepG2 cells transduced with lentivirus containing GPR146 expression plasmid were cultured in the presence of 100 ng/ml Doxycycline for 48 hours, washed in ice-cold PBS once and then fixed in ice-cold methanol for 20 minutes. After being rinsed in ice-cold PBS twice, the cells were blocked in PBST (PBS supplemented with 0.1% Triton X-100) containing 5% bovine serum albumin for 1 hour, followed by incubation with primary and secondary antibodies.

Gene expression analysis—Total RNA was extracted from mouse tissues or cells using RNeasy kit (QIAGEN) or Trizol reagent (Invitrogen). 1 μg of RNA was applied for reverse transcription with using Maxima H Minus cDNA synthesis system (Thermo). Quantitative real-time PCR (RT-PCR) was performed on a ViiA™ 7 RT-PCR system (Applied Biosystems Inc.). Melting curve analysis was carried out to confirm the RT-PCR products. Expression data is presented after calculating the relative expression level compared to the housekeeping gene RPLP0. Primer sequences used in this study are listed in Table S2.

RNA quality was verified using the Agilent Bioanalyzer and the 6000 nano kit. Genome-wide mRNA expression profiles in mouse liver were performed using microarray analysis with the Affymetrix GeneChip™ Mouse Gene 2.1 ST Array Strip, according to the manufacturer's instructions. Gene set enrichment analysis was performed based on the protocol previously reported(Subramanian et al., 2005). In brief, the list of pre-ranked genes

Author Manuscript Author Manuscript Author Manuscript Author Manuscript

from microarray analysis was then analyzed for reactome pathway gene sets, hallmark gene sets and KEGG gene sets. Significantly enriched terms were identified using a false discovery rate *q* value of less than 0.05.

Plasmids—Human GPR146 with or without a c-terminal FLAG tag was cloned from MGC human GPR146 sequence-verified cDNA (Clone ID: 4563636) into pDONOR211 (Invitrogen) through a gateway cloning strategy (Invitrogen). GPR146 open reading frame was further transferred to FU-tetO-Gateway (Addgene) vector to generate doxycycline-inducible GPR146 recombinant expression vector FU-tetO-GPR146 or FU-tetO-GPR146CFLAG.

Fecal lipids analysis—Fecal lipids were extracted using Folch's extraction procedure(Folch et al., 1957) with further optimizations. Briefly, 50 mg of dried, pulverized feces from individually housed mice were re-suspended in 200 μl of PBS, mixed with 1200 μl of 2:1 chloroform-methanol (v/v) and further vortexed vigorously for 30 seconds. 100 μl of PBS was then added into the mixture and further vortexed for 15 seconds. Afterwards, the mixture was centrifuged at 4,200 × g for 10 minutes at 4 degree, and 200 μl of the organic layer was transferred into a new tube to dry, followed by resuspension in 100 μl of 1% Triton X-100 in ethanol. The suspension was further dried using a SpeedVac vacuum concentrator before dissolving in 100 μl of 1% Triton X-100 in PBS. TG and TC levels were measured using Infinity Triglycerides Reagent (Thermo Fisher) and Infinity Cholesterol Reagent (Thermo Fisher) respectively according to the manufacturer's instructions.

Hepatic lipid content assay—The protocol for hepatic lipid extraction is adapted from previously published paper(Lee et al., 2011) with slight modifications. Briefly, to measure the lipid (Triglyceride and cholesterol) levels of liver, snap-frozen liver samples were weighed and homogenized in ten volume of ice-cold PBS. Two-hundred microliters of the homogenate was transferred into 1,200 ul of chloroform: methanol (2:1; v/v) mixture followed by vigorous vortex for 30 seconds. One-hundred microliters of ice-cold PBS was then added into the mixture and mixed vigorously for 15 seconds. The mixture was then centrifuged at 4,200 rpm for 10 minutes at 4 degree. Two-hundred microliters of the organic phase (bottom layer) was transferred into a new tube and evaporated for dryness. Two-hundred microliters of 1% Triton X-100 in ethanol was used to dissolve the dried lipid with constant rotation for 2 hours. Triglyceride and cholesterol content were determined using the Infinity Triglycerides reagent (Thermo Scientific) and Infinity Cholesterol reagent (Thermo Scientific) respectively, based on manufacturer's instructions.

QUANTIFICATION AND STATISTICAL ANALYSIS

All immunoblotting quantifications were conducted in ImageJ. No statistical methods were used to predetermine sample size. Values are presented with mean ± SD or mean ± SEM, as indicated in figure legends. Statistical analyses were performed using Prism (Graphpad). Statistical significance of differences was determined by unpaired, two-tailed Student's t test (two groups), or one-way ANOVA with Tukey post hoc analysis (more than two groups), with corrected *p values* < 0.05 considered statistically significant. Asterisks denote corresponding statistical significance $*p < 0.05$ and $**p < 0.01$. The type of statistical tests

Author Manuscript Author Manuscript Author Manuscript Author Manuscript

performed and definition of “n” are indicated in the figure legends. For cell culture ELISA, qPCR and western blotting, each sample within each biological replicate corresponds to one well from a tissue culture plate. For mouse liver western blotting, each sample corresponds to protein extract from one mouse.

DATA AND CODE AVAILABILITY

The accession number for the microarray datasets reported in this paper is GEO: GSE139082.

Supplementary Material

Refer to Web version on PubMed Central for supplementary material.

ACKNOWLEDGEMENTS

We express our gratitude to Jorge Plutzky for project discussion. We thank Lin Wu at Genome Modification Facility in Harvard University for generating *Gpr146*$^{-/-}$ and *Gpr146*$^{fl/fl}$ mice. We thank Curtis R. Warren and Max Friesen for generating the Doxycycline-inducible expression plasmid. We thank Shunsuke Katsuki for sharing the protocol of atherosclerosis analysis. We also thank Junghyun Lee and Yujia Shen for proofreading the manuscript.

This work was funded by the National Institutes of Health (NHLBI/R33HL120781 and NIDDK/R01DK097768 to C.A.C.), the Nutrition Obesity Research Center of Harvard (P30DK040561 to C.A.C. and A.A.S.), the Netherlands CardioVascular Research Initiative and the Established Investigator of the Netherlands Heart Foundation (CVON2017-2020; 2015T068 to J.A.K.) and Institut de France-Fondation Lefoulon-Delalande Postdoctoral Fellowship (to A.R.).

REFERENCES

Addis RC, Hsu FC, Wright RL, Dichter MA, Coulter DA, and Gearhart JD (2011). Efficient conversion of astrocytes to functional midbrain dopaminergic neurons using a single polycistronic vector. PLoS One 6, e28719. [PubMed: 22174877]

Adiels M, Olofsson SO, Taskinen MR, and Boren J (2008). Overproduction of very low-density lipoproteins is the hallmark of the dyslipidemia in the metabolic syndrome. Arterioscler Thromb Vasc Biol 28, 1225–1236. [PubMed: 18565848]

Ai M, Otokozawa S, Asztalos BF, Ito Y, Nakajima K, White CC, Cupples LA, Wilson PW, and Schaefer EJ (2010). Small dense LDL cholesterol and coronary heart disease: results from the Framingham Offspring Study. Clin Chem 56, 967–976. [PubMed: 20431054]

Arito M, Horiba T, Hachimura S, Inoue J, and Sato R (2008). Growth factor-induced phosphorylation of sterol regulatory element-binding proteins inhibits sumoylation, thereby stimulating the expression of their target genes, low density lipoprotein uptake, and lipid synthesis. J Biol Chem 283, 15224–15231. [PubMed: 18403372]

Barrows BR, and Parks EJ (2006). Contributions of different fatty acid sources to very low-density lipoprotein-triacylglycerol in the fasted and fed states. J Clin Endocrinol Metab 91, 1446–1452. [PubMed: 16449340]

Brown MS, and Goldstein JL (1975). Regulation of the activity of the low density lipoprotein receptor in human fibroblasts. Cell 6, 307–316. [PubMed: 212203]

Brown MS, and Goldstein JL (1986). A receptor-mediated pathway for cholesterol homeostasis. Science 232, 34–47. [PubMed: 3513311]

Cuchel M, Bruckert E, Ginsberg HN, Raal FJ, Santos RD, Hegele RA, Kuivenhoven JA, Nordestgaard BG, Descamps OS, Steinhagen-Thiessen E, et al. (2014). Homozygous familial hypercholesterolaemia: new insights and guidance for clinicians to improve detection and clinical management. A position paper from the Consensus Panel on Familial Hypercholesterolaemia of the European Atherosclerosis Society. Eur Heart J 35, 2146–2157. [PubMed: 25053660]

Author Manuscript Author Manuscript Author Manuscript Author Manuscript

Defesche JC, Gidding SS, Harada-Shiba M, Hegele RA, Santos RD, and Wierzbicki AS (2017). Familial hypercholesterolaemia. Nat Rev Dis Primers 3, 17093. [PubMed: 29219151]

Do R, Willer CJ, Schmidt EM, Sengupta S, Gao C, Peloso GM, Gustafsson S, Kanoni S, Ganna A, Chen J, et al. (2013). Common variants associated with plasma triglycerides and risk for coronary artery disease. Nat Genet 45, 1345–1352. [PubMed: 24097064]

Folch J, Lees M, and Sloane Stanley GH (1957). A simple method for the isolation and purification of total lipides from animal tissues. J Biol Chem 226, 497–509. [PubMed: 13428781]

Fremin C, Ezan F, Boisselier P, Bessard A, Pages G, Pouyssegur J, and Baffet G (2007). ERK2 but not ERK1 plays a key role in hepatocyte replication: an RNAi-mediated ERK2 knockdown approach in wild-type and ERK1 null hepatocytes. Hepatology 45, 1035–1045. [PubMed: 17393467]

Gokey NG, Lopez-Anido C, Gillian-Daniel AL, and Svaren J (2011). Early growth response 1 (Egr1) regulates cholesterol biosynthetic gene expression. J Biol Chem 286, 29501–29510. [PubMed: 21712389]

Goldstein JL, and Brown MS (1973). Familial hypercholesterolemia: identification of a defect in the regulation of 3-hydroxy-3-methylglutaryl coenzyme A reductase activity associated with overproduction of cholesterol. Proc Natl Acad Sci U S A 70, 2804–2808. [PubMed: 4355366]

Graf GA, Yu L, Li WP, Gerard R, Tuma PL, Cohen JC, and Hobbs HH (2003). ABCG5 and ABCG8 are obligate heterodimers for protein trafficking and biliary cholesterol excretion. J Biol Chem 278, 48275–48282. [PubMed: 14504269]

Guegan JP, Fremin C, and Baffet G (2012). The MAPK MEK1/2-ERK1/2 Pathway and Its Implication in Hepatocyte Cell Cycle Control. Int J Hepatol 2012, 328372. [PubMed: 23133759]

Hegele RA (2009). Plasma lipoproteins: genetic influences and clinical implications. Nat Rev Genet 10, 109–121. [PubMed: 19139765]

Hokanson JE, and Austin MA (1996). Plasma triglyceride level is a risk factor for cardiovascular disease independent of high-density lipoprotein cholesterol level: a meta-analysis of population-based prospective studies. J Cardiovasc Risk 3, 213–219. [PubMed: 8836866]

Horton JD, Bashmakov Y, Shimomura I, and Shimano H (1998). Regulation of sterol regulatory element binding proteins in livers of fasted and refed mice. Proc Natl Acad Sci U S A 95, 5987–5992. [PubMed: 9600904]

Horton JD, Goldstein JL, and Brown MS (2002). SREBPs: activators of the complete program of cholesterol and fatty acid synthesis in the liver. J Clin Invest 109, 1125–1131. [PubMed: 11994399]

Ivanova EA, Myasoedova VA, Melnichenko AA, Grechko AV, and Orekhov AN (2017). Small Dense Low-Density Lipoprotein as Biomarker for Atherosclerotic Diseases. Oxid Med Cell Longev 2017, 1273042. [PubMed: 28572872]

Klarin D, Damrauer SM, Cho K, Sun YV, Teslovich TM, Honerlaw J, Gagnon DR, DuVall SL, Li J, Peloso GM, et al. (2018). Genetics of blood lipids among ~300,000 multi-ethnic participants of the Million Veteran Program. Nat Genet 50, 1514–1523. [PubMed: 30275531]

Kotzka J, Lehr S, Roth G, Avci H, Knebel B, and Muller-Wieland D (2004). Insulin-activated Erk-mitogen-activated protein kinases phosphorylate sterol regulatory element-binding Protein-2 at serine residues 432 and 455 in vivo. J Biol Chem 279, 22404–22411. [PubMed: 14988395]

Kotzka J, Muller-Wieland D, Roth G, Kremer L, Munck M, Schurmann S, Knebel B, and Krone W (2000). Sterol regulatory element binding proteins (SREBP)-1a and SREBP-2 are linked to the MAP-kinase cascade. J Lipid Res 41, 99–108. [PubMed: 10627507]

Lee JM, Lee YK, Mamrosh JL, Busby SA, Griffin PR, Pathak MC, Ortlund EA, and Moore DD (2011). A nuclear-receptor-dependent phosphatidylcholine pathway with antidiabetic effects. Nature 474, 506–510. [PubMed: 21614002]

Liang G, Yang J, Horton JD, Hammer RE, Goldstein JL, and Brown MS (2002). Diminished hepatic response to fasting/refeeding and liver X receptor agonists in mice with selective deficiency of sterol regulatory element-binding protein-1c. J Biol Chem 277, 9520–9528. [PubMed: 11782483]

Liu DJ, Peloso GM, Yu H, Butterworth AS, Wang X, Mahajan A, Saleheen D, Emdin C, Alam D, Alves AC, et al. (2017). Exome-wide association study of plasma lipids in >300,000 individuals. Nat Genet 49, 1758–1766. [PubMed: 29083408]

Author Manuscript Author Manuscript Author Manuscript Author Manuscript

Matsuda M, Korn BS, Hammer RE, Moon YA, Komuro R, Horton JD, Goldstein JL, Brown MS, and Shimomura I (2001). SREBP cleavage-activating protein (SCAP) is required for increased lipid synthesis in liver induced by cholesterol deprivation and insulin elevation. Genes Dev 15, 1206–1216. [PubMed: 11358865]

Moon YA, Liang G, Xie X, Frank-Kamenetsky M, Fitzgerald K, Koteliansky V, Brown MS, Goldstein JL, and Horton JD (2012). The Scap/SREBP pathway is essential for developing diabetic fatty liver and carbohydrate-induced hypertriglyceridemia in animals. Cell Metab 15, 240–246. [PubMed: 22326225]

Ozaki KI, Awazu M, Tamiya M, Iwasaki Y, Harada A, Kugisaki S, Tanimura S, and Kohno M (2016). Targeting the ERK signaling pathway as a potential treatment for insulin resistance and type 2 diabetes. Am J Physiol Endocrinol Metab 310, E643–E651. [PubMed: 26860984]

Rader DJ (2016). New Therapeutic Approaches to the Treatment of Dyslipidemia. Cell Metab 23, 405–412. [PubMed: 26853751]

Rong S, Cortes VA, Rashid S, Anderson NN, McDonald JG, Liang G, Moon YA, Hammer RE, and Horton JD (2017). Expression of SREBP-1c Requires SREBP-2-mediated Generation of a Sterol Ligand for LXR in Livers of Mice. Elife 6.

Sanjana NE, Shalem O, and Zhang F (2014). Improved vectors and genome-wide libraries for CRISPR screening. Nat Methods 11, 783–784. [PubMed: 25075903]

Slakey LL, Craig MC, Beytia E, Briedis A, Feldbruegge DH, Dugan RE, Qureshi AA, Subbarayan C, and Porter JW (1972). The effects of fasting, refeeding, and time of day on the levels of enzymes effecting the conversion of -hydroxy- -methylglutaryl-coenzyme A to squalene. J Biol Chem 247, 3014–3022. [PubMed: 4337504]

Subramanian A, Tamayo P, Mootha VK, Mukherjee S, Ebert BL, Gillette MA, Paulovich A, Pomeroy SL, Golub TR, Lander ES, et al. (2005). Gene set enrichment analysis: a knowledge-based approach for interpreting genome-wide expression profiles. Proc Natl Acad Sci U S A 102, 15545–15550. [PubMed: 16199517]

Teslovich TM, Musunuru K, Smith AV, Edmondson AC, Stylianou IM, Koseki M, Pirruccello JP, Ripatti S, Chasman DI, Willer CJ, et al. (2010). Biological, clinical and population relevance of 95 loci for blood lipids. Nature 466, 707–713. [PubMed: 20686565]

van Biesen T, Luttrell LM, Hawes BE, and Lefkowitz RJ (1996). Mitogenic signaling via G protein-coupled receptors. Endocr Rev 17, 698–714. [PubMed: 8969974]

Wang H, Yang H, Shivalila CS, Dawlaty MM, Cheng AW, Zhang F, and Jaenisch R (2013). One-step generation of mice carrying mutations in multiple genes by CRISPR/Cas-mediated genome engineering. Cell 153, 910–918. [PubMed: 23643243]

Westra HJ, Peters MJ, Esko T, Yaghootkar H, Schurmann C, Kettunen J, Christiansen MW, Fairfax BP, Schramm K, Powell JE, et al. (2013). Systematic identification of trans eQTLs as putative drivers of known disease associations. Nat Genet 45, 1238–1243. [PubMed: 24013639]

Willer CJ, Schmidt EM, Sengupta S, Peloso GM, Gustafsson S, Kanoni S, Ganna A, Chen J, Buchkovich ML, Mora S, et al. (2013). Discovery and refinement of loci associated with lipid levels. Nat Genet 45, 1274–1283. [PubMed: 24097068]

Yang H, Wang H, Shivalila CS, Cheng AW, Shi L, and Jaenisch R (2013). One-step generation of mice carrying reporter and conditional alleles by CRISPR/Cas-mediated genome engineering. Cell 154, 1370–1379. [PubMed: 23992847]

Yu L, Hammer RE, Li-Hawkins J, Von Bergmann K, Lutjohann D, Cohen JC, and Hobbs HH (2002). Disruption of Abcg5 and Abcg8 in mice reveals their crucial role in biliary cholesterol secretion. Proc Natl Acad Sci U S A 99, 16237–16242. [PubMed: 12444248]

Zhernakova DV, Deelen P, Vermaat M, van Iterson M, van Galen M, Arindrarto W, van ‘t Hof P, Mei H, van Dijk F, Westra HJ, et al. (2017). Identification of context-dependent expression quantitative trait loci in whole blood. Nat Genet 49, 139–145. [PubMed: 27918533]

Author Manuscript Author Manuscript Author Manuscript Author Manuscript

Highlights

1. GPR146 regulates plasma cholesterol levels in both human and mouse
2. Reduced hepatic SREBP2 activity and VLDL secretion rate in the absence of GPR146
3. GPR146 regulates SREBP2 signaling pathway through ERK1/2
4. GPR146 deficiency protects against atherosclerosis in *Ldlr*−/− mice

Author Manuscript Author Manuscript Author Manuscript Author Manuscript

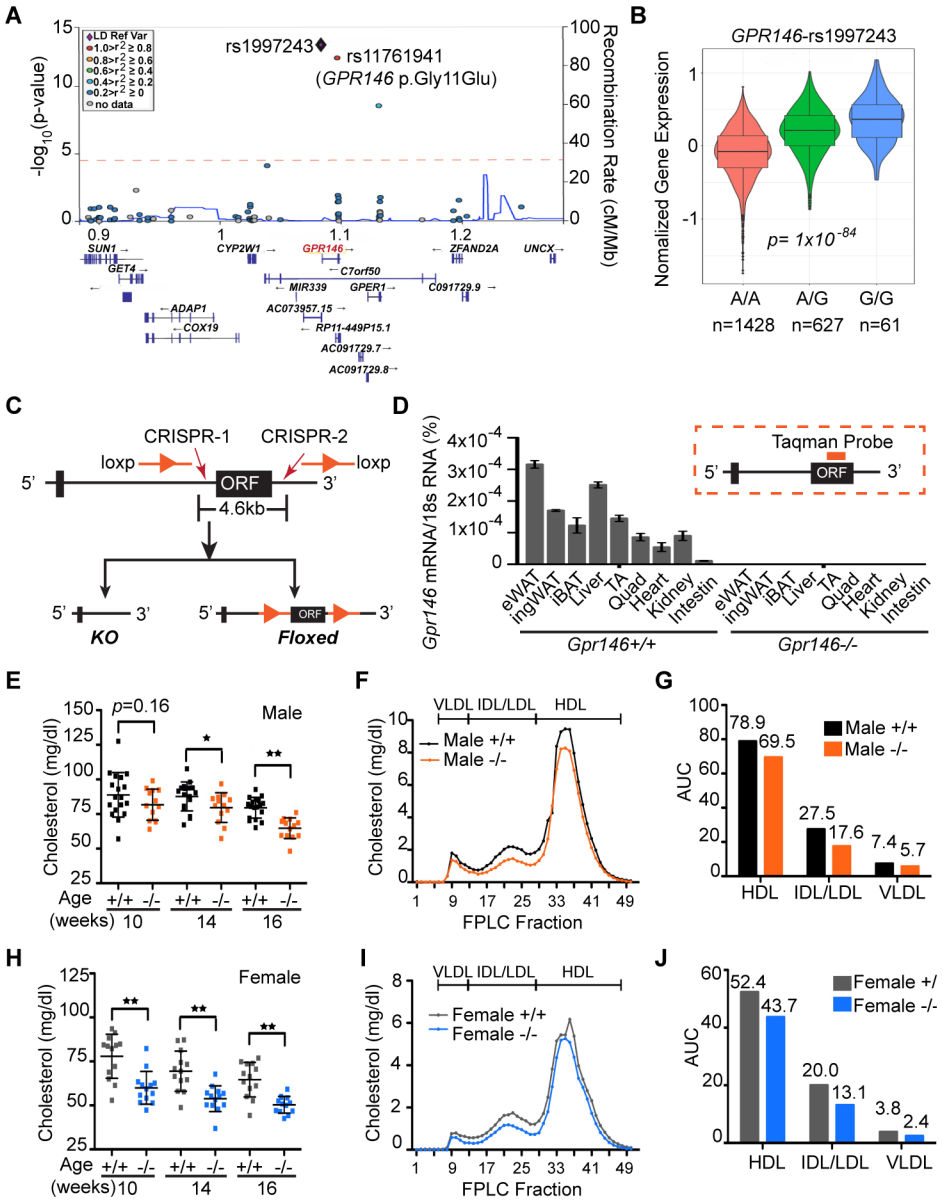

Figure 1. GPR146 Regulates Plasma Cholesterol Levels in both Human and Mouse

(A) Reginal (7p22 locus) association of GWAS variants with plasma cholesterol levels shows that common SNP rs1997243 (purple diamond) and *GPR146* p.Gly11Glu (red circle) are significantly associated with plasma TC levels in humans.

(B) eQTL studies using 2,116 human blood samples revealed a highly significant dose-dependent relation between the rs1997243 G-allele and *GPR146* expression (n=1428 for A/A, n=627 for A/G and n=61 for G/G).

(C) Schematic diagram showing generation of *Gpr146* whole-body knockout ($Gpr146^{-/-}$) and floxed mouse models ($Gpr146^{fl/fl}$) using CRISPR/Cas9 system.

(D) *Gpr146* mRNA levels in epididymal white adipose tissue (eWAT), inguinal white adipose tissue (ingWAT), interscapular brown adipose tissue (iBAT), liver, skeletal muscle

Author Manuscript Author Manuscript Author Manuscript Author Manuscript

tibialis anterior (TA), quadriceps (Quad), heart, kidney and intestine, of 8-weeks old *Gpr146* wild type (+/+) and knockout (−/−) male mice (n=3 mice per group).

(E and H) Plasma total cholesterol (TC) levels of 16-hour fasted male (E) and female (H) *Gpr146* wild-type (+/+) mice and knockout (−/−) littermates fed chow at different ages indicated (n= 13–18 mice per group, by Student's *t*-test).

(F and I) Pooled plasma from male (F) and female (I) mice was subjected to Fast Protein Liquid Chromatography (FPLC) analysis, and cholesterol was measured in each of the eluted fractions (pooled samples of n=13–18 mice per group).

(G and J) Area under curve (AUC) was used to calculate the levels of VLDL-C (fractions 7 to 13), IDL/LDL-C (fraction 13 to 29) and HDL-C (fraction 29 to 49) in FPLC plots (F and I).

* $p< 0.05$, ** $p< 0.01$; bars in E and H indicate mean ± s.d.; bars in D indicate mean± s.e.m.

Author Manuscript Author Manuscript Author Manuscript Author Manuscript

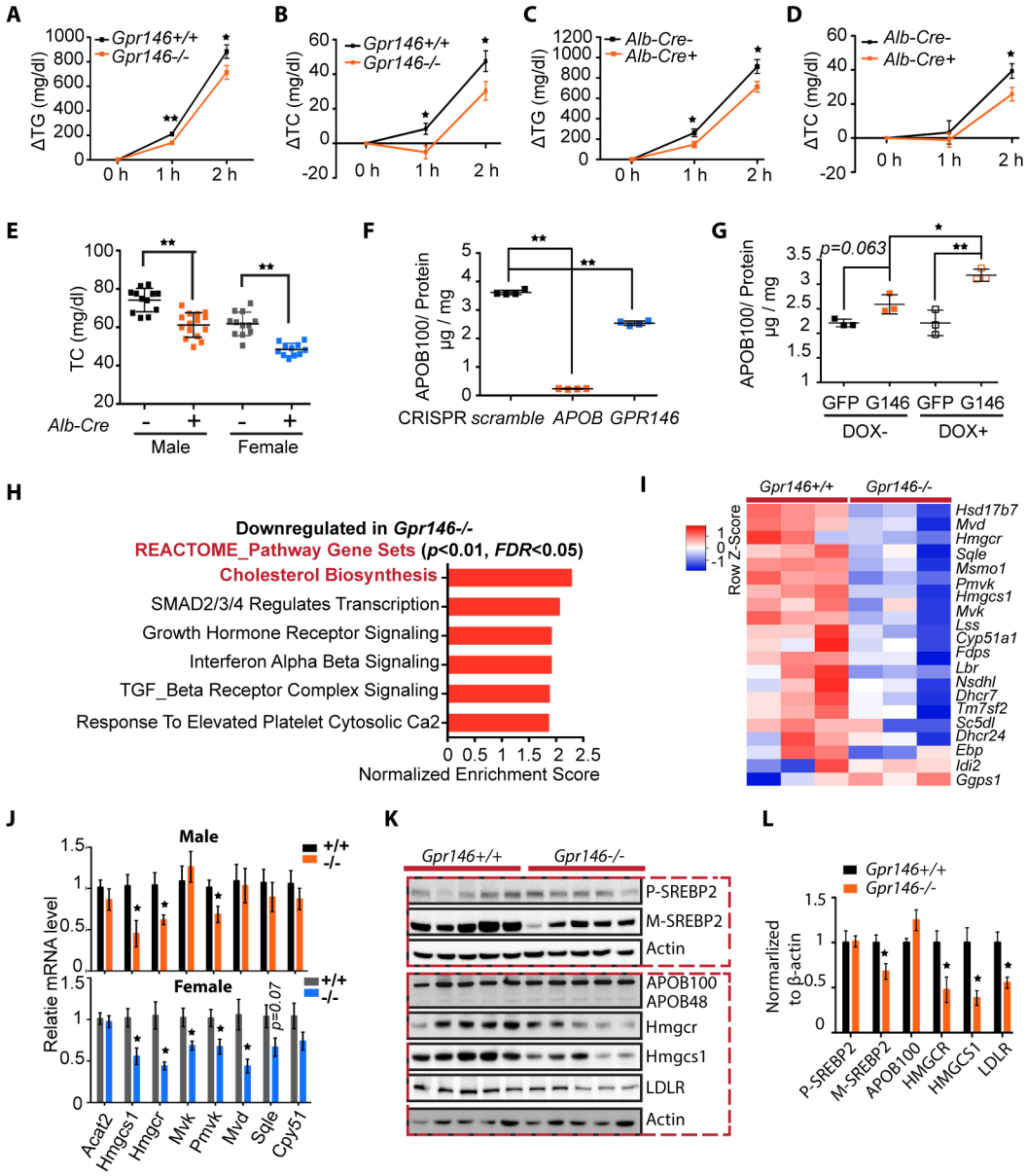

Figure 2. GPR146 Deficiency Reduces Hepatic SREBP2 Activities and VLDL Secretion Rate

(A-D) Changes of plasma TG (A and C) and TC (B and D) after Poloxamer-407 injection in *Gpr146* whole body knockout mice (*Gpr146*$^{+/+}$ vs *Gpr146*$^{-/-}$, n=12–14 mice per group, by Student's *t*-test) and liver-specific knockout mice (*Alb-Cre-* vs *Alb-Cre+*, n=8 mice per group, by Student's *t*-test) fed chow.

(E) Plasma TC levels of 16-hour fasted male and female *Gpr146* liver-specific knockout (*Alb-Cre+)* and control littermates (*Alb-Cre-)* fed chow (n= 11–15 mice per group, by Student's *t*-test).

(F) Depletion of GPR146 via CRISPR/Cas9 leads to reduced APOB100 secretion in Huh7 human hepatoma cells (n=4 replicates per genotype per experiment, representative of 3 independent experiments, by Student's *t*-test).

Author Manuscript Author Manuscript Author Manuscript Author Manuscript

(G) Recombinantly overexpressed GPR146, compared with GFP control, results in increased APOB100 secretion (n=3 replicates per genotype per experiment, representative of 2 independent experiments, by one-way ANOVA).
(H) Top ranking REACTOME pathway gene sets discovered from gene set enrichment analysis (GSEA) of genes that are differentially expressed in liver of male *Gpr146*$^{+/+}$ mice and *Gpr146*$^{-/-}$ littermates (n=3 mice per group) upon 6-hour refeeding after a 16-hour fast.
(I) Heat map of cholesterol biosynthesis (REACTOME Pathway Database)-related genes in livers of male *Gpr146*$^{+/+}$ and *Gpr146*$^{-/-}$ mice (n=3 mice per group).
(J) Quantitative polymerase chain reaction (qPCR) expression analysis of cholesterol biosynthetic genes in liver of 6-hour refed male and female *Gpr146*$^{+/+}$ mice and *Gpr146*$^{-/-}$ littermates (n=5 mice per group, by Student's *t*-test).
(K and L) Western blot (K) and relative quantification (L) of SREBP2 precursor (P-SREBP2), mature SREBP2 (M-SREBP2), APOB100, HMGCR, HMGCS1 and LDLR in liver of 6-hour refed male *Gpr146*$^{+/+}$ mice and *Gpr146*$^{-/-}$ littermates (n=5 mice per group, by Student's *t*-test).
* $p < 0.05$, ** $p < 0.01$; bars in A-D, J and L indicate mean± s.e.m., bars in E-G indicate mean ± s.d..

Author Manuscript Author Manuscript Author Manuscript Author Manuscript

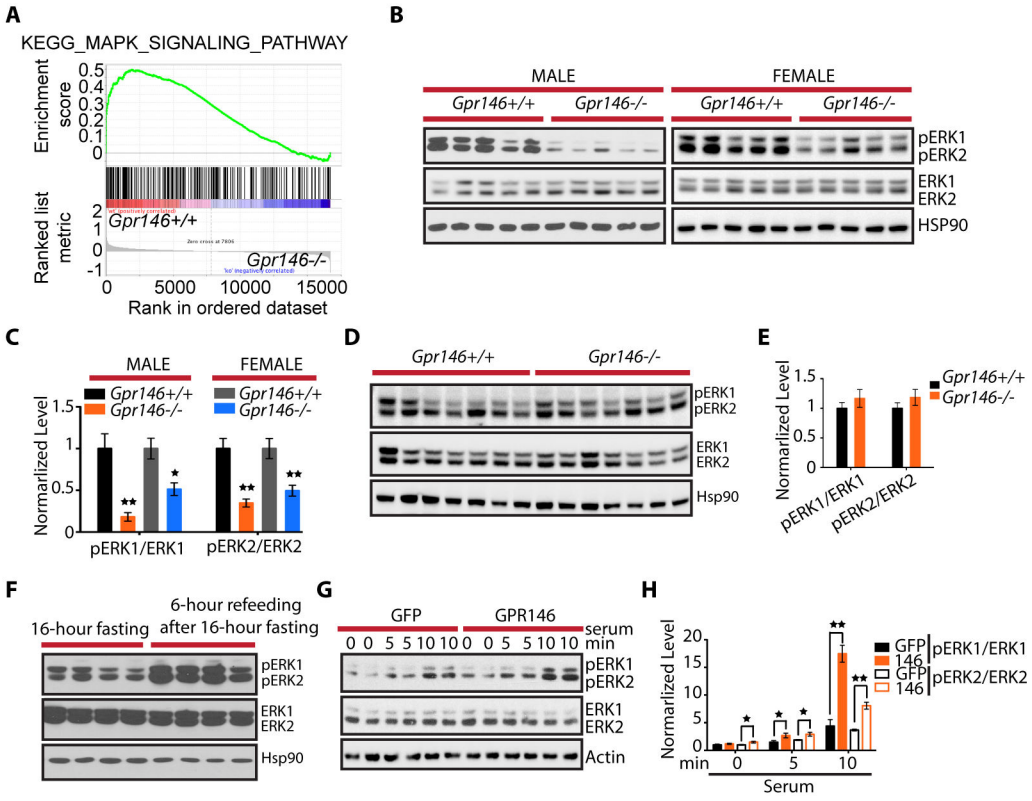

Figure 3. GPR146 Promotes ERK1/2 Activities in Hepatocytes Upon Feeding

(A) GSEA enrichment plot of MAPK_Signaling gene set (KEGG pathway database) in liver of *Gpr146*$^{+/+}$ mice and *Gpr146*$^{-/-}$ littermates (n=3 mice per group) upon 6-hour refeeding after a 16-hour fast.

(B and C) Western blot (B) and relative quantification (C) of phosphorylated ERK1/2 (pERK1/2) and total ERK1/2 in liver of 6-hour refed *Gpr146*$^{+/+}$ mice and *Gpr146*$^{-/-}$ littermates (n=5 mice per group, by Student's *t*-test).

(D and E) Western blot (D) and relative quantification (E) of phosphorylated ERK1/2 (pERK1/2) and total ERK1/2 in liver of 16-hour fasted *Gpr146*$^{+/+}$ mice and *Gpr146*$^{-/-}$ littermates (n=7 mice per group, by Student's *t*-test).

(F) Western blot of phosphorylated ERK1/2 (pERK1/2) and total ERK1/2 in liver of 16-hour fasted male mice (C57BL/6J) or 6-hour refed littermates upon chow diet feeding (n=4 mice per group).

(G and H) Western blot (G) and relative quantification (H) showing upregulated pERK1/2 levels with recombinant expression of human GPR146 in HepG2 cells upon stimulation with serum for the time indicated (n=2 replicates per genotype per experiment, representative of 3 independent experiments, by Student's *t*-test).

* $p < 0.05$, ** $p < 0.01$; bars in C indicate mean± s.e.m., bars in E and H indicate mean ± s.d..

Author Manuscript Author Manuscript Author Manuscript Author Manuscript

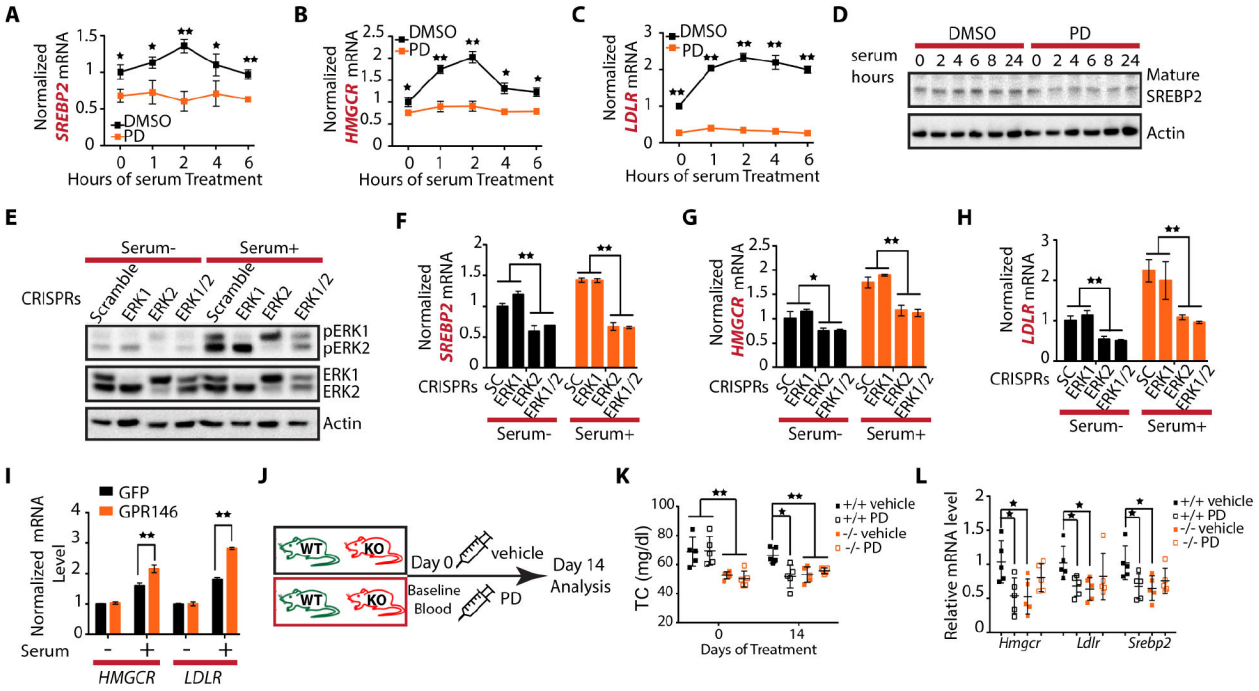

Figure 4. GPR146 Regulates SREBP2 Signaling Pathway and Plasma TC levels through ERK1/2 upon Feeding

(A-C) Fold induction of *SREBP2* (A), *HMGCR* (B) *and LDLR* (C) mRNA levels in human hepatoma HepG2 cells upon serum stimulation in the presence or absence of MEK inhibitor PD0325901 (PD) (n=3 replicates per time point per experiment, representative of 3 independent experiments, by Student's *t*-test).

(D) Western blot of mature SREBP2 in HepG2 cells upon serum stimulation in the presence or absence of PD0325901.

(E) Western blot showing CRISPR-induced depletion of ERK1, ERK2 or ERK1/2 in HepG2 cells in the presence or absence of serum stimulation.

(F-H) Fold induction of *SREBP2* (F), *HMGCR* (G) *and LDLR* (H) mRNA levels in HepG2 cells lacking ERK1, ERK2 or ERK1/2 (n=3 replicates per genotype per experiment, representative of 3 independent experiments, by one-way ANOVA).

(I) Fold induction of *HMGCR and LDLR* mRNA level in HepG2 cells with recombinant expression of GPR146 or GFP (n=3 replicates per genotype per experiment, representative of 3 independent experiments, by Student's *t*-test).

(J) Schedule of MEK inhibitor PD0325901 treatment *in vivo*.

(K and L) Plasma TC levels (K) and relative mRNA levels of hepatic *Hmgcr, Ldlr and Srebp2* (L) in chow-fed female *Gpr146*$^{+/+}$ mice and *Gpr146*$^{-/-}$ littermates upon 6-hour refeeding after a 16-hour fast, treated with vehicle or PD0325901 (5mg/kg Body Weight) for the period of time indicated (n=5 mice per group, by one-way ANOVA).

* $p < 0.05$, ** $p < 0.01$; bars in this figure indicate mean± s.d..

Author Manuscript Author Manuscript Author Manuscript Author Manuscript

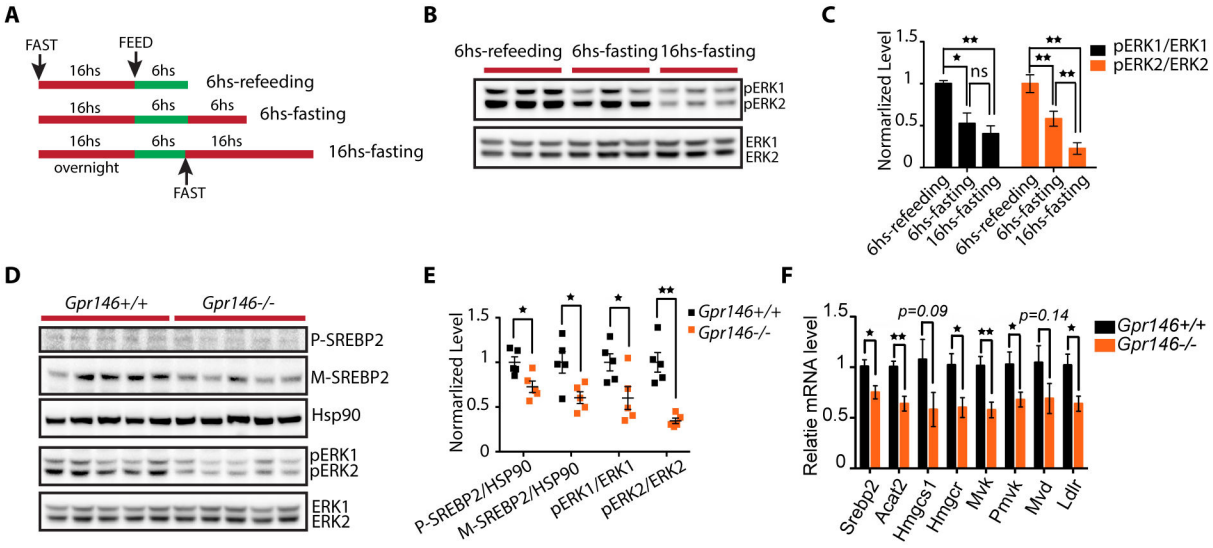

Figure 5. GPR146 Regulates ERK/SREBP2 Axis in Mice upon Short Period of Fasting

(A) Schedule of fasting and refeeding treatment *in vivo*.

(B and C) Western blot (B) and relative quantification (C) of phosphorylated ERK1/2 (pERK1/2) and total ERK1/2 in livers of mice upon different fasting refeeding regimens (n=3 mice per group, by one-way ANOVA).

(D and E) Western blot (D) and relative quantification (E) of SREBP2 precursor (P-SREBP2), mature SREBP2 (M-SREBP2), pERK1/2 and total ERK1/2 in livers of 6-hour fasted $Gpr146^{+/+}$ mice and $Gpr146^{-/-}$ littermates (n=5 mice per group, by Student's *t*-test).

(F) Quantitative polymerase chain reaction (qPCR) expression analysis of cholesterol biosynthetic genes in liver of 6-hour fasted $Gpr146^{+/+}$ mice and $Gpr146^{-/-}$ littermates (n=5 mice per group, by Student's *t*-test).

* $p< 0.05$, ** $p< 0.01$; bars in C and E indicate mean± s.d., bars in F indicate mean± s.e.m..

Author Manuscript
Author Manuscript
Author Manuscript
Author Manuscript

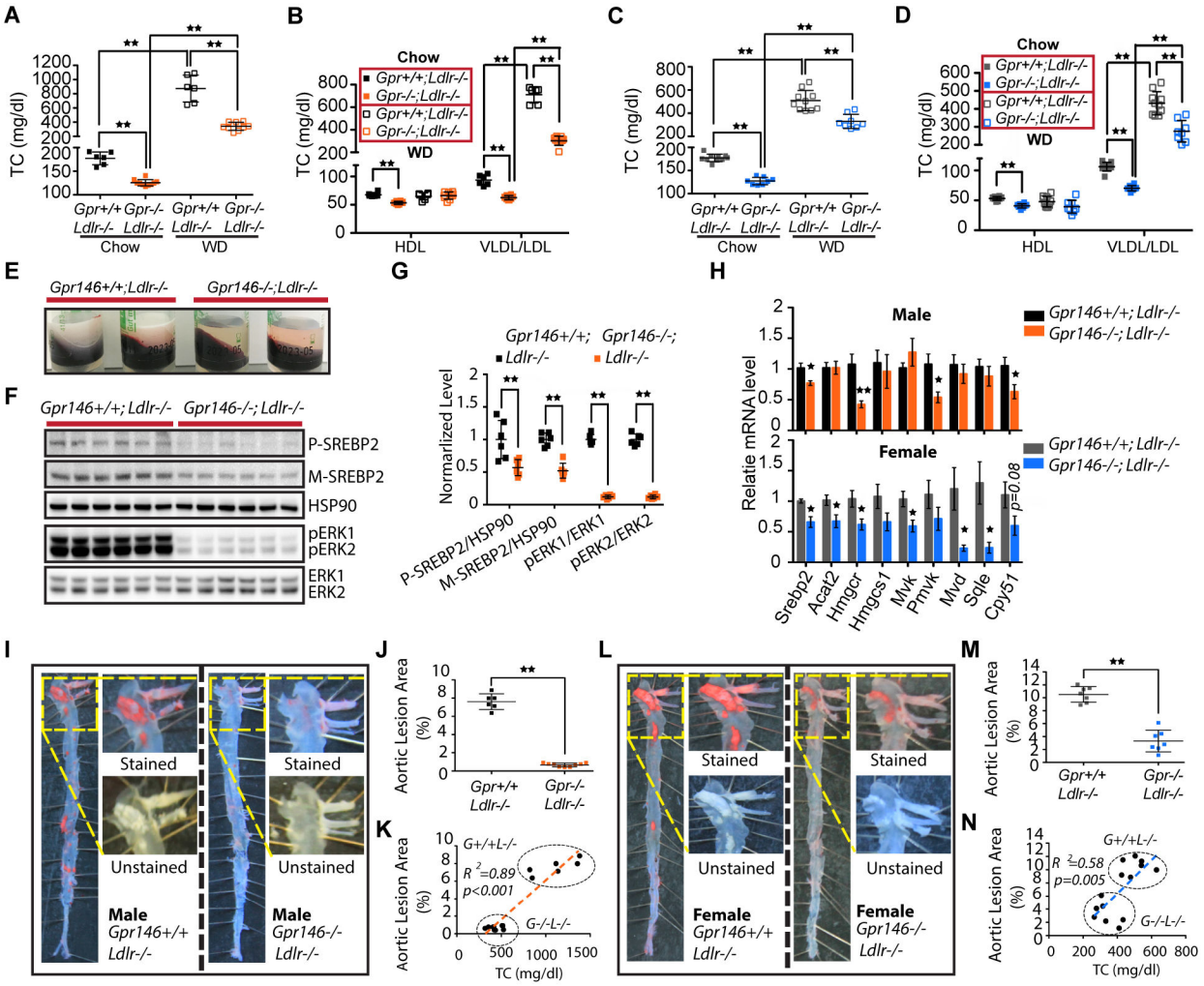

Figure 6. GPR146 Deficiency Protects Against Hypercholesterolemia and Atherosclerosis in LDLR-deficient Mice

(A and C) Plasma TC levels of *Gpr146* whole-body knockout male (A) and female (C) mice lacking LDLR fed chow or western diet (WD) for 16 weeks (n=6–10 mice per group, by one-way ANOVA).

(B and D) HDL and VLDL/LDL fractions in plasma of *Gpr146* whole-body knockout male (B) and female (D) mice lacking LDLR were separated, and cholesterol levels were measured in both fractions (n=6–10 mice per group, by one-way ANOVA).

(E) Representative images of plasma (top layer) isolated from $Gpr146^{+/+}$ and $Gpr146^{-/-}$ male mice lacking LDLR fed WD for 16 weeks.

(F and G) Western blot (F) and relative quantification (G) of SREBP2 precursor (P-SREBP2), mature SREBP2 (M-SREBP2), pERK1/2 and total ERK1/2 in livers of 6-hour refed male $Gpr146^{+/+}$ mice and $Gpr146^{-/-}$ littermates lacking LDLR upon chow feeding (n=6 mice per group, by Student's *t*-test).

(H) Quantitative polymerase chain reaction (qPCR) expression analysis of cholesterol biosynthetic genes in liver of 6-hour refed male and female $Gpr146^{+/+}$ mice and $Gpr146^{-/-}$ littermates lacking LDLR upon chow feeding (n=6–7 mice per group, by Student's *t*-test).

Author Manuscript Author Manuscript Author Manuscript Author Manuscript

(I and L) Representative images of aortas before and after Oil Red O staining in *Gpr146* wild type and whole-body knockout male (I) and female (L) mice lacking LDLR fed WD for 16 weeks.

(J and M) Quantification of aortic lesion areas (expressed as a percentage of the lumen area in full-length aorta) in male (J) and female (M) mice (n=6–10 mice per group, by Student's *t*-test).

(K and N) Scatter plot of plasma total cholesterol levels and aortic lesion areas in male (K) and female mice (N) lacking LDLR.

* $p < 0.05$, ** $p < 0.01$; bars in A-D, G, J and M indicate mean± s.d., bars in H indicate mean ± s.e.m..

Author Manuscript Author Manuscript Author Manuscript Author Manuscript

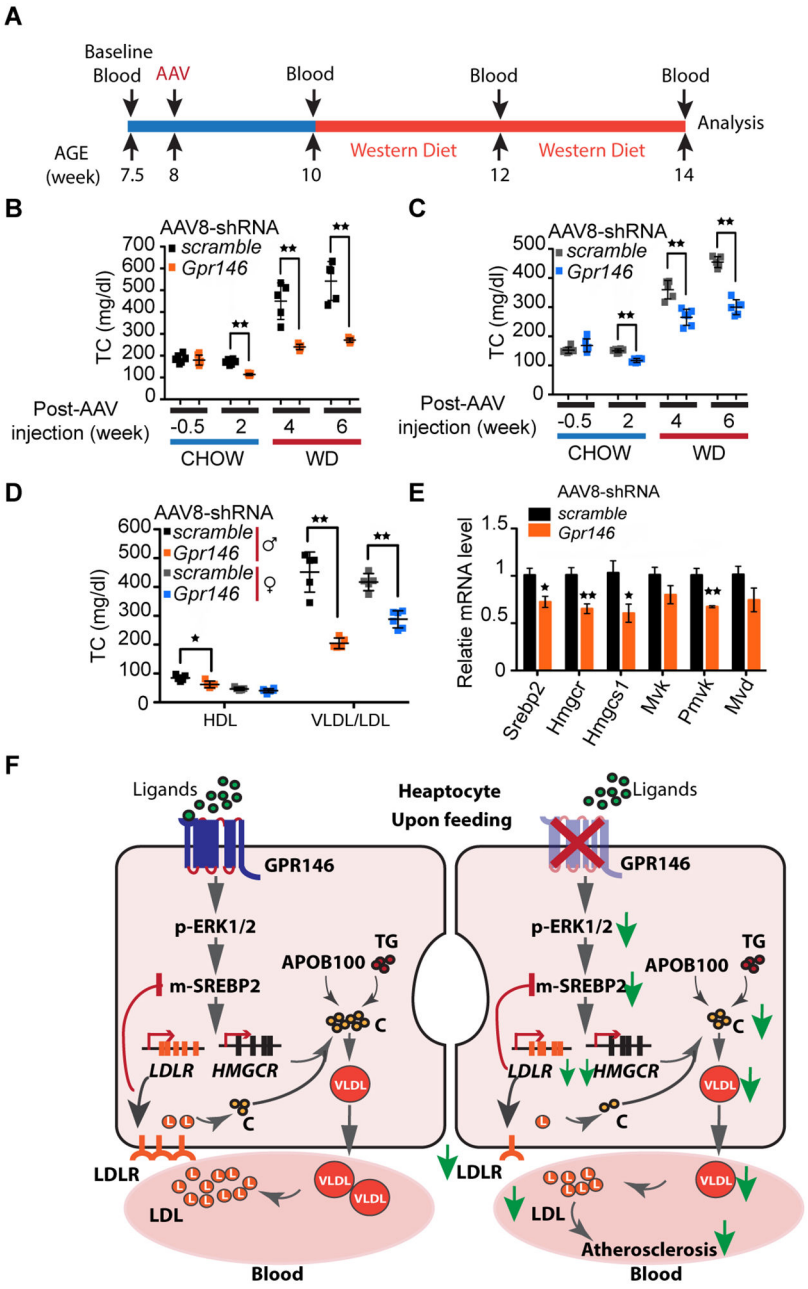

Figure 7. Knockdown of GPR146 by AAV-delivered shRNA Lowers Plasma Cholesterol Levels in Mice Lacking LDLR

(A) Schedule of AAV-mediated knockdown of GPR146 in mice lacking LDLR.

(B and C) Plasma TC levels of male (B) and female (C) mice lacking LDLR before and after injection of AAV8-scramble control or AAV8-Gpr146-shRNA viruses (n=5–6 mice per group, by Student's *t*-test).

(D) HDL and VLDL/LDL fractions in plasma of LDLR-deficient mice 6-weeks post AAV injection were separated, and cholesterol levels were measured in both fractions (n=5–6 mice per group, by Student's *t*-test).

Author Manuscript Author Manuscript Author Manuscript Author Manuscript

(E) qPCR expression analysis of cholesterol biosynthetic genes in liver of 6-hour refed male LDLR-deficient mice 6-weeks post AAV injection (n=5–6 mice per group, by Student's *t*-test).

(F) Model of the pathway by which depletion of hepatic GPR146 protects against hypercholesterolemia and atherosclerosis.

* $p < 0.05$, ** $p < 0.01$; bars in B-D indicate mean± s.d., bars in E indicate mean± s.e.m..

Author Manuscript Author Manuscript Author Manuscript Author Manuscript

Key Resource Table

REAGENT or RESOURCE
Antibodies
Mouse monoclonal anti-HSP90
Mouse monoclonal anti-APOB
Rabbit monoclonal anti-p44/42 MAPK (Erk1/2)
Rabbit monoclonal anti-p38 MAPK
Rabbit polyclonal anti-SAPK/JNK
Rabbit monoclonal anti-phospho-p44/42 MAPK (Erk1/2) (Thr202/Tyr204)
Rabbit polyclonal anti-phospho-p38 MAPK (Thr180/Tyr182)
Rabbit monoclonal anti-phospho-SAPK/JNK (Thr183/Tyr185)
Rabbit monoclonal anti-HMGCS1
Rabbit polyclonal anti-SREBP2
Rabbit polyclonal anti-HMGCR
Rabbit polyclonal anti-LDLR
Mouse monoclonal anti-β-actin
Mouse monoclonal anti-FLAG
Bacterial and Virus Strains
AAV8-GFP-U6-scrmb-shRNA
AAV8-GFP-U6-rm-Gpr146-shRNA
Chemicals, Peptides, and Recombinant Proteins
PD0325901
Poloxamer-407
Low Density Lipoprotein from Human Plasma, Dil Complex
Critical Commercial Assays
Infinity Triglycerides Reagent

Author Manuscript Author Manuscript Author Manuscript Author Manuscript

REAGENT or RESOURCE
Infinity Cholesterol Reagent
HDL and LDL/VLDL Quantitation Kit
Human ApoB ELISAPRO kit
Deposited Data
Microarray Raw data
Experimental Models: Cell Lines
Human: HEK293T
Human: Huh7
Human: HepG2
Mouse: AML12
Experimental Models: Organisms/Strains
Mouse: C57BL/6J
Mouse: B6.Cg-*Speer6-ps1*$^{Tg(Alb\text{-}cre)21Mgn}$/J
Mouse: B6; FVB-Tg(Adipoq-cre)1Evdr/J
Mouse: B6. 129S7-*Ldlr*^{tm1Her}/J
Mouse: *Gpr146*$^{-/-}$
Mouse: *Gpr146*$^{fl/fl}$
Mouse: *Gpr146-LKO*
Mouse: *Gpr146-FKO*
Mouse: *Gpr146*$^{-/-}$/ *Ldlr*$^{-/-}$
Oligonucleotides
Gpr146 sgRNA1 targeting sequence: GCTACCTTTTGGCACGGGTT
Gpr146 sgRNA2 targeting sequence: GTGGCTAAGGGATTATATGG
loxp ssDNA template1: TGACCCACCAGAGAGGCTTTTGTGTGCCTTCCTGTGCCACTACTCCACCAGGAGCAGAGCTGCTGCTACCTTTTGGCACGATAACTTCGTATAATGTATGCTATACG
loxp ssDNA template2: GAGTTTGAATCTAAGCCCAGATGCACAGACCTTGTTTCAAGTCAAAGTCTTCAGGGCTGCAAAAGTGGCTAAGGGATTATGAGCTCATAACTTCGTATAGCATACAT
Gpr146 AAV8-shRNA targeting sequence: GCATTATCTGGGCATCCTACA
see Table S2 for additional oligonucleotides
Recombinant DNA
Human GPR146 cDNA

Author Manuscript

Author Manuscript

Author Manuscript

Author Manuscript

REAGENT or RESOURCE
Plasmid: lentiCas9-Blast
Plasmid: lentiGuide-Puro
Plasmid: FU-tetO-Gateway
Plasmid: FU-tetO-GPR146
Plasmid: FU-tetO-GPR146-FLAG
Plasmid: FU-tetO-eGFP-FLAG
Software and Algorithms
ImageJ
GraphPad Prism5